



Particulate emissions from cooking activities: emission factors, emission dynamics, and mass spectrometric analysis for different preparation methods

Julia Pikmann¹, Frank Drewnick¹, Friederike Fachinger¹, Stephan Borrmann^{1,2}

5 ¹Particle Chemistry Department, Max Planck Institute for Chemistry, Mainz, 55128, Germany

²Institute for Atmospheric Physics, Johannes Gutenberg University Mainz, Mainz, 55128, Germany

Correspondence to: Frank Drewnick (frank.drewnick@mpic.de)

Abstract.

As most people, especially in developed countries, spend most of their time indoors, they are strongly exposed to indoor aerosol, which potentially can lead to adverse health effects. A major source of indoor aerosols are cooking activities releasing large amounts of particulate emissions, both number and mass wise, with often complex composition. To investigate the characteristics of cooking emissions and parameters, which influence these characteristics, we conducted a comprehensive study in form of a measurement series cooking 19 dishes with different ingredients and preparation methods. The emissions were monitored in real time with multiple online instruments measuring physical and chemical particle properties as well as trace gas concentrations. With the same instrumentation, the influence of cooking emissions on the ambient aerosol load was studied at two German Christmas markets.

For six variables, we observed changes during the cooking: particle number concentration of smaller (particle diameter $d_p > 5$ nm) and larger particles ($d_p > 250$ nm), PM (PM_1 , $PM_{2.5}$, PM_{10}), BC, PAH and organics mass concentrations. Generally, similar emission characteristics were observed for dishes with the same preparation method mainly due to similar cooking temperature and use of oil. The emission dynamics of the above-mentioned variables as well as the sizes of emitted particles were mostly influenced by the cooking temperature and activities during cooking. The emissions were quantified via emission factors, with the highest values for grilled dishes, one to two orders of magnitude smaller ones for oil-based cooking (baking, stir-frying, deep-frying) and the smallest for boiled dishes.

For the identification of cooking emissions with the Aerodyne aerosol mass spectrometer (AMS) and generally the identification of new AMS markers, we propose a new diagram type where the variability of the mass spectra of different aerosols is considered. Combining our results and those from previous studies for quantification of cooking-related organic aerosol with the AMS, we recommend using values for the relative ionization efficiency which are larger than the default value for organics ($RIE_{org} = 1.4$): for rapeseed oil-based cooking 2.17 ± 0.48 and for soy oil-based cooking 5.16 ± 0.77 .

1 Introduction

Aerosols influence the earth's climate as well as air quality and human health (IPCC, 2021; WHO, 2021). According to calculations of the WHO (World Health Organization) air pollution leads to 6.7 million premature deaths every year and almost half of them were attributed to indoor air pollution (WHO, 2022). People tend to spend an increasing fraction of their time indoors, especially in developed countries with about 90%; they are therefore exposed over long periods to the indoor aerosol and the therein contained pollutants (Diffey, 2011; Goldstein et al., 2021; Liu et al., 2022). Inhaled, these pollutants can cause the formation of radicals leading to oxidative stress and formation of oxygenated species which can induce inflammation processes (Kreyling et al., 2006).



The resulting impacts on health are versatile and include respiratory diseases, cardiovascular diseases, allergies, infectious diseases, and cancer (Pope et al., 2004; Pope and Dockery, 2006; Shiraiwa et al., 2017; Xu et al., 2022).

The composition of the indoor aerosol is influenced by the atmospheric aerosol infiltrating through ventilation and leaks as well as by multiple emission sources indoors (Abbatt and Wang, 2020; Marval and Tronville, 2022). Aerosols can be generated through evaporation of substances from furnishing, building materials, and consumer products. The human body itself is a direct and indirect source of aerosols due to perspiration, breathing, talking etc. Furthermore, different activities at home (like cleaning and moving around) lead to resuspension and emission of aerosol particles. Combustion processes like cigarette smoking, candle or wood burning also cause strong indoor emissions (Abbatt and Wang, 2020).

Cooking is considered one of the most important indoor sources, an activity which often occurs on a daily basis at home as well as on larger scales in e.g. restaurants. In a study evaluating the personal exposure to indoor aerosol, cooking was identified as the largest contributor to indoor PM (particulate matter) (Zhao et al., 2006). The indoor PM concentrations can increase tremendously depending on the cooking activity with PM_{2.5} concentrations (PM of aerodynamic diameter with $d_p < 2.5 \mu\text{m}$) of up to $1400 \mu\text{g m}^{-3}$ (Abdullahi et al., 2013). In developing countries where solid fuels are often used for cooking the health burden through the stronger emissions is even higher (Chafe et al., 2014; Martin et al., 2021; Nasir and Colbeck, 2013).

Cooking activities also have an impact on the ambient aerosol. In urban areas cooking contributes 5-30% of the organic aerosol in fine particles during the typical meal times, as shown by various measurements, including measurements with the AMS (aerosol mass spectrometer; Crippa et al., 2013; Mohr et al., 2012; Struckmeier et al., 2016), TAG (thermal desorption aerosol gas chromatography–mass spectrometry; Wang et al., 2020) and filter measurements (Rogge et al., 1991). During mapping measurements in the proximity of restaurants, performed by Robinson et al. (2018) with an AMS, most measured organic aerosol plumes were attributed to cooking emissions with concentrations of up to $100 \mu\text{g m}^{-3}$, showing the potential of cooking emissions to affect local air quality.

During cooking, a large fraction of the emitted particle mass is in fine particles (PM_{2.5}), while the particle number concentrations of the emissions are dominated by ultrafine particles ($d_p < 100 \text{ nm}$). Accordingly, the number and mass size distributions are dominated by Aitken and accumulation mode particles, respectively (Buonanno et al., 2009; Marval and Tronville, 2022; Wallace et al., 2004; Wallace and Ott, 2011; Yeung and To, 2008). When inhaled, these particles can enter deep into the lungs to the alveoli. Especially the ultrafine particles, due to their larger specific surface, can cause stronger reactions or inflammation processes in the body, compared to larger particles with the same total mass (Baron et al., 2011; Marval and Tronville, 2022; Thomas, 2013).

A large variety of substances is emitted during cooking including volatile organic compounds and particulate matter. The major constituents are saturated and unsaturated fatty acids, glycerides, as well as sugars and their decomposition products, like levoglucosan. Furthermore, aromatics, PAHs (polycyclic aromatic hydrocarbons), and aldehydes might be emitted, many of which are hazardous to health (Abdullahi et al., 2013; Cheng et al., 2016; Klein et al., 2016; Liu et al., 2018; Zhao et al., 2007; Zhao et al., 2019).

Studies of individual aspects of emissions from cooking activities have shown that the composition and quantity of the emissions are affected by various parameters, like the preparation method, ingredients, cooking temperature, and used fuel type (e.g., Zhang et al., 2010). The particle sizes as well as number and mass concentrations increase with increasing temperature during cooking (Amouei Torkmahalleh et al., 2012; Buonanno et al., 2009; Klein et al., 2016; Zhang et al., 2010). The comparison of different preparation methods like steaming, boiling, baking, deep-frying, stir-frying, and grilling showed that the lowest emissions were observed from steaming and boiling while the strongest were from grilling, followed by deep- and stir-frying (Alves et al., 2015; Lee et al., 2001; Olson and Burke, 2006). The differences are mainly due to the different cooking temperatures and the use of oil. For example, See and Balasubramanian (2006) measured the particle size distribution of emissions from cooking tofu with five



different preparation methods and observed a 24-fold increase in particle number concentration compared to the background during deep-frying compared to a 1.5-fold increase during steaming. Another aspect which is relevant for the amount of particulate emissions is the smoke point of the used oil. Studies measuring the emissions from heating different oils showed that for oils with high smoke points, as sunflower and soy oil, compared to olive oil with a lower smoke point, the emissions were 4 – 9 times lower (Amouei Torkmahalleh et al., 2012; Gao et al., 2013).

The analysis of cooking emissions is challenging due to the high complexity of the emitted substance mixture as well as the high emission dynamics with strong variability in concentrations during the cooking. Especially the ingredients and preparation method have a strong influence on the emissions (Abdullahi et al., 2013; Maré et al., 2018; Zhang et al., 2010). So far, there are few systematic studies covering the influence of different cooking parameters on the emissions while measuring a large variety of chemical and physical aerosol properties in parallel.

Therefore, we conducted a comprehensive study of cooking emissions by performing a measurement series cooking 19 dishes with different ingredients and preparation methods. During the cooking, various chemical and physical properties were monitored in real time with our mobile laboratory (MoLa, used in stationary measurement mode in the laboratory), including PM, organics and non-refractory inorganics, BC and PAH mass concentrations as well as the particle number concentration and size distribution. These online measurements allowed for the analysis of the emission dynamics during the cooking and of the influence of different cooking activities during the preparation on the emissions.

The emissions were quantified and emission factors related to the amount of food were determined for all relevant variables. Based on the laboratory measurements, we investigated how the identification of cooking emissions with the AMS and generally the identification of new AMS markers can be further improved using a new diagram type. Furthermore, the influence of cooking emissions on ambient aerosol was studied at two German Christmas markets with MoLa. Based on these measurements, we examined the applicability of the laboratory-derived emission factors to ambient data.

2 Methods and instrumentation

2.1 Laboratory study design and experimental procedure

For a systematic study, 19 different dishes were cooked in the laboratory (Table 1). The concept was to prepare dishes often-cooked in Central Europe (Germany) while including different classes of ingredients and preparation methods, i.e. boiling, stir-frying, deep-frying, baking, and grilling with gas and charcoal. Each dish was cooked with an amount for approximately four persons and all ingredients were weighed before preparation (Table S1). Rapeseed oil was used for the preparation of all dishes except for the boiled dishes, frozen pizza, and brownies. Only salt and pepper were used as seasoning if not stated otherwise in Table S1.

Table 1: List of prepared dishes for the laboratory study (for details see Table S1).

| Preparation method | Dishes |
|----------------------------|--|
| Boiling | Boiled potatoes, rice, noodles |
| Stir-frying | Fried potatoes, bratwurst, schnitzel, fish, spaghetti Bolognese, stir-fried vegetables, Indian curry |
| Deep-frying | French fries (in pot), French fries (deep fryer), Bavarian doughnut (in pot) |
| Baking | Baked potatoes, frozen pizza, brownies |
| Grilling on gas grill | Steaks, vegetable skewers |
| Grilling on charcoal grill | Steaks |



Each dish was cooked three times on the same day to assess the variability of the emissions due to variations in ingredients and performance of the cooking process between the repetitions. Background measurements were performed over 20 min right before the start of the cooking. Between repetitions, we waited for the aerosol concentration to return to a stable background level; if necessary, the room was ventilated. The cooking process was recorded using a webcam (HD Pro Webcam C920, Logitech, Switzerland) to apportion individual concentration changes to activities during the cooking. Furthermore, the temperature of the cooked food and of the cookware was measured repeatedly with an IR thermometer (Fluke 568, Fluke Corporation, USA). During the baking experiments, the temperature inside the oven was monitored continuously using the same thermometer with a thermocouple as sensor.

The measurements were performed in an experimental hall with a custom-made kitchen setup consisting of a regular household electric stove with oven (30540 P, Privileg, Germany) and a fume hood above (CH 44060-60 GA, Respekta®, Germany) which was connected to an exhaust ventilation (Fig.1). The exhaust flow rate Q_E was $7.5 \text{ m}^3 \text{ min}^{-1}$. To quantitatively capture the cooking emissions, the space between the stove and the fume hood was encased by four plexiglass walls and only the front glass was left partially open, leaving a gap of ca. 50 cm to be able to access the cookware. For the oven and barbecue experiments, additional screens were used for a complete capture of the emissions. From the pipe of the exhaust ventilation above the fume hood the cooking emissions were sub-sampled, diluted (1:13) with a dilution system (VKL 10 E, Palas, Germany) using dry, particle-free compressed air (1 bar), and transferred to the instruments inside our mobile laboratory MoLa. As the dilution with dry air led to low relative humidity ($< 7 \%$) we measured dry particles, which might differ in particle size (and, therefore, mass) from particles measured without dilution close to the source. The particle loss within the setup was calculated using the particle loss calculator (von der Weiden et al., 2009) and found to be negligible for the particle size range relevant in this study.

The stir-fried dishes were prepared in a Teflon-coated frying pan, the boiled dishes in a stainless-steel pot, and the deep-fried dishes in a stainless-steel pot or a deep fryer (FT 2400.9, 2300 W, 2.5 L oil, Tevion, Germany). For the barbecue experiments, a gas and a charcoal grill were used.

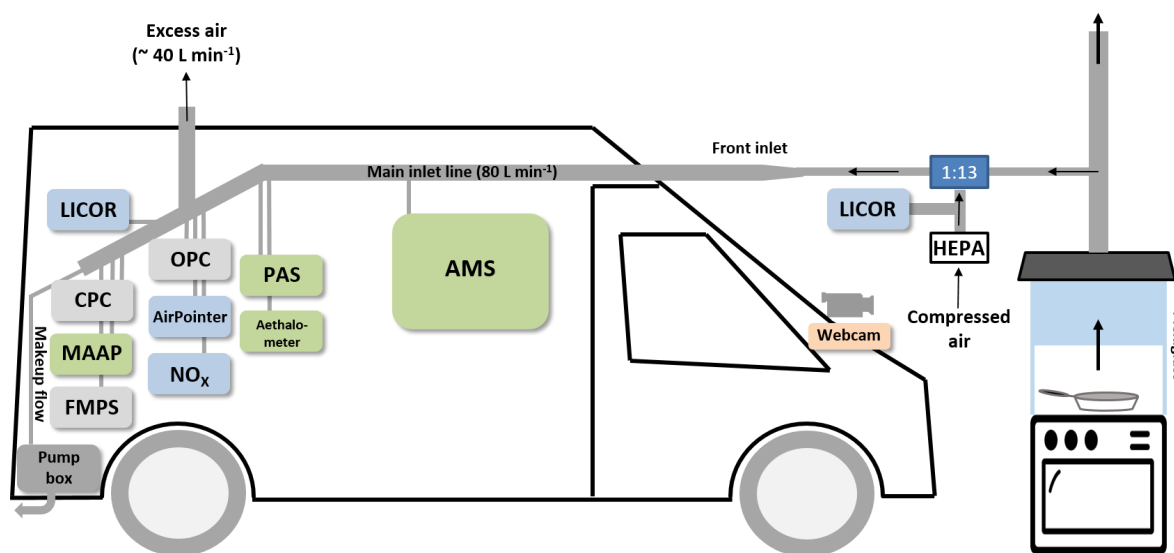


Figure 1: Scheme of the laboratory setup for the cooking experiments (MoLa scheme adapted from Drewnick et al., 2012). HEPA: high-efficiency particulate air filter. For details regarding the instrumentation, see Table S2.



2.2 Ambient measurements at two German Christmas markets

Measurements to assess the influence of cooking emissions on the local air quality under ambient conditions were performed at
135 two Christmas markets in Germany:

- Ingelheim (05.12. until 08.12.2019)

The Christmas market in Ingelheim (ca. 35000 inhabitants) was located around the Burgkirche; the mobile laboratory MoLa was situated directly behind a circle of seven food stands, offering burgers, French fries, flame-grilled salmon, waffles, vegan food, and mulled wine, at the eastern edge of the market. A barrel for wood fire was placed on the 07. and
140 08.12.2019 at a distance of 25 m from MoLa and another barrel in the middle of the food stands circle next to MoLa (distance approximately 10 m) during all evenings. More food stands and wood fire barrels were distributed over the market, which covered an area of ca. 100 m by 50 m. The opening hours were 06.12. 5 PM until 10 PM, 07.12. 3 PM until 10 PM, and 08.12. 3 PM until 9 PM.

- Bingen (13.12. until 15.12.2019)

The Christmas market in Bingen (ca. 25000 inhabitants) was spread over the city center. MoLa was located at the eastern edge of the Bürgermeister Neff Square, an open area of ca. 50 m by 25 m, with the closest food stand at a distance of 25 m. The six food stands on the square, offering Langos, French fries, bratwurst, barbecue, crepes, raclette, tarte flambée, sweets, and mulled wine, were arranged in a half circle. On the 14.12. a suckling pig was grilled over an open wood fire next to the western edge of the square. Furthermore, on the 14. and 15.12. a barrel for wood fire was placed in the middle
150 of the square and another barrel on a crossing road at the western edge of the square. The opening hours were 13.12. 4 PM until 9 PM, 14.12. 11 AM until 9 PM, and 15.12. 11 AM until 7 PM.

The inlet height for the MoLa instrumentation was at 5 m above ground level. We measured mostly dry particles as the elevated temperature within MoLa led to low relative humidity (< 32 %) in the inlet lines. During the measurements in Ingelheim, we additionally measured with a portable aethalometer (microAeth® MA200, AethLabs, USA) the black carbon mass concentrations
155 during random walks across the market.

The temperatures during the measurements at both locations were in the range of 4 – 11 °C and light occasional rain showers occurred. The wind direction in Ingelheim was mainly from south-southwest with wind speeds of 1 – 4 m s⁻¹ and in Bingen from west with wind speeds of 0.5 – 2 m s⁻¹.

2.3 Instrumentation

160 Within the mobile laboratory MoLa various instruments were used to measure different aerosol properties like the particle number concentration (measured with a condensation particle counter CPC for particles with $d_p > 5$ nm and with an optical particle counter OPC for particles with $d_p > 250$ nm) and particle size distribution ($d_p = 5.6$ nm – 32 μm, measured with two different instruments: the fast mobility particle sizer FMPS and the OPC), the mass concentration for the fractions PM₁, PM_{2.5}, PM₁₀ and the chemical components black carbon (BC) and PAH in the PM₁ fraction as well as trace gas concentrations of NO_x, O₃, SO₂, CO, and CO₂.

165 The HR-ToF-AMS (high-resolution time-of-flight aerosol mass spectrometer) was applied to measure the non-refractory chemical composition of PM₁ and was operated in V-mode for maximum sensitivity, with a time resolution of 15 s for the laboratory measurements and 30 s for the Christmas market measurements. An overview of the MoLa instruments, the measured variables, time resolutions, and measurement uncertainties is provided in Table S2; for further details regarding MoLa see Drewnick et al. (2012).



170 2.4 Data processing

All data processing was performed with Igor Pro (versions 6 – 8, WaveMetrics, Inc., USA). The data from the laboratory (Christmas market) measurements were averaged on a common 15 s (30 s) time base. All data were corrected for sampling time delays, checked for invalid data due to e.g. internal calibrations, and normalized to standard conditions ($T = 20\text{ °C}$, $p = 1013.25\text{ hPa}$). In the further analysis of the cooking experiments, the sampling dilution (1:13) was considered. From the combined FMPS and OPC size distribution data the PM_{10} , $\text{PM}_{2.5}$, and PM_{10} mass concentrations were calculated (SI Sect. S1). The time averaged data from the individual experiments were averaged over the three repetitions (if not stated otherwise), such that the corresponding standard deviation reflects the variability between the repetitions. For the Christmas market measurements, the periods with opened and closed market, respectively, were averaged separately over all days.

To calculate the cooking emissions from the laboratory data, the averaged background concentrations (c_{Back}) measured before each experiment were subtracted from the concentrations measured during the cooking (c_{Cook}). Identified trends in the background concentrations were corrected accordingly. Emission factors (EF) were calculated to estimate the total emissions from cooking per kilogram food according to Eq. (1) from the average concentration of the respective variable ($c_{\text{Avg}} = c_{\text{Cook}} - c_{\text{Back}}$), the volume flow rate of the exhaust Q_E ($7.5\text{ m}^3\text{ min}^{-1}$), the preparation time t , the dilution factor D (13), and the mass of the ingredients m .

$$EF = \frac{c_{\text{Avg}} \cdot Q_E \cdot t \cdot D}{m} \quad (1)$$

The analysis of the high-resolution AMS data was performed with the software tools SQUIRREL 1.63I and PIKA 1.23I within Igor Pro following the standard procedures (Canagaratna et al., 2007). The ionization efficiency of the AMS as well as the relative ionization efficiencies for ammonium (4.21) and sulfate (1.31) were determined in calibrations before and after the measurements. For the laboratory data, a collection efficiency (CE) of 1 was applied as we assumed that the emitted particles were liquid, and for each dish the relative ionization efficiency for organics (RIE_{COA}) was determined separately (see Sect. 3.1.4). For the Christmas market data, the standard values for the CE (0.5) and RIE_{Org} (1.4) were applied (Canagaratna et al., 2007) except for the cooking organic aerosol fraction, as described in Sect. 3.5.1.

For comparison of measured mass spectra with the ones of different organic aerosol types from previous studies (Table 2), mass spectra were taken from the AMS spectra database (Ulbrich et al., 2009; Ulbrich et al., 2022), as listed in Table S3.

Positive matrix factorization (PMF, Paatero and Tapper, 1994) was performed on the AMS organic high resolution mass spectra up to m/z 116 using the PMF Evaluation Tool (PET) v3.07C (Ulbrich et al., 2009, see SI Sect. S2 for details).



Table 2: List of organic aerosol types and their acronyms.

| Acronym | Aerosol type |
|-----------|--|
| COA | Cooking organic aerosol |
| BBOA | Biomass burning organic aerosol |
| HOA | Hydrocarbon-like organic aerosol |
| OOA | Oxygenated organic aerosol |
| LVOOA | Low-volatile oxygenated organic aerosol |
| SVOOA | Semi-volatile oxygenated organic aerosol |
| LOOOA | Less oxidized oxygenated organic aerosol |
| MOOOA | More oxidized oxygenated organic aerosol |
| NOA | Nitrogen-enriched organic aerosol |
| CCOA | Coal combustion organic aerosol |
| CSOA | Cigarette smoke-related organic aerosol |
| IEPOX-SOA | Isoprene-epoxydiol-derived secondary organic aerosol |

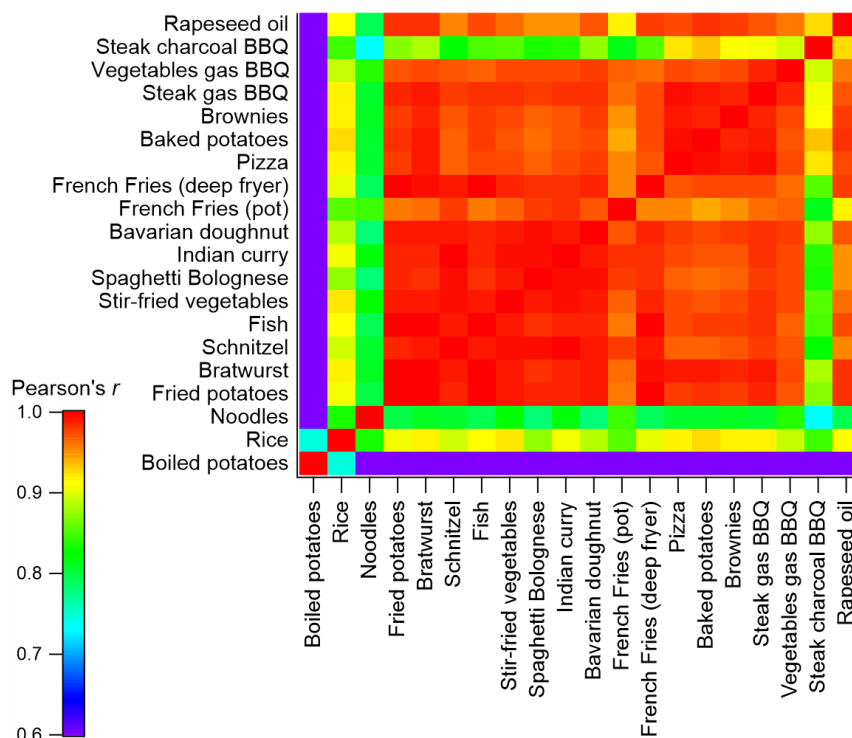
3 Results and discussion

3.1 Chemical analysis of cooking emissions with HR-ToF-AMS

200 3.1.1 Average chemical composition and correlation of mass spectra

The mass spectra of the non-refractory PM₁ cooking emissions from different dishes show high similarity between each other. On average, the measured aerosol consisted mainly of organics (96.7 – 99.9 %) with minor contributions of nitrate (< LOD – 2.8 %), ammonium (< LOD – 0.5 %), sulfate (< LOD – 1.8 %), and chloride (< LOD – 0.4 %). Most ions of the organic fraction were attributed to the C_xH_y family (77.8 – 91.8 %) indicating a weakly oxidized aerosol. The remaining ions were mostly oxygen containing ions (C_xH_yO₁: 6.5 – 17.4 %; C_xH_yO_{>1}: < LOD – 6.2 %) with a small fraction attributed to the C_xH_yN family (< LOD – 2.3 %) and C_x family (0.1 – 0.8 %). For two dishes, Indian curry and spaghetti Bolognese, small fractions of the ions were attributed to the C_xS family (0.1 %) and also the sulfate fraction was slightly elevated (0.3 – 0.7 %), presumably due to the emission of sulfur-containing substances from onions in the food (Boelens et al., 1971).

To obtain quantitative information on how similar the emissions from different experiments are, linear correlations between the averaged normalized organic mass spectra (unit mass resolution) of the emissions from all dishes were calculated (Fig. 2). Additionally, the mass spectrum of emissions from heated rapeseed oil (Fig. S1) was included in this analysis as rapeseed oil was used for all dishes where oil was required. Most spectra show a high similarity between each other and with the spectrum of rapeseed oil (Pearson's $r > 0.94$), and we conclude that the emissions consisted mostly of vaporized and re-condensed oil. Consistently, the mass spectra of emissions from boiled dishes and steaks grilled with charcoal are less similar to those of the rest: For the boiled dishes no oil was used and for the steaks the mass spectrum is strongly influenced by the emissions from the charcoal itself. Additionally, the correlations of the cooking mass spectra with the ones of various fatty acids (palmitic, stearic, oleic, and linoleic acid), all measured with the AMS (Ulbrich et al., 2022, not shown in Fig. 2) show the highest similarity with the one of oleic acid ($r = 0.85 - 0.94$), the main component of rapeseed oil.



220 **Figure 2: Linear correlation of the averaged mass spectra of cooking emissions for all laboratory experiments and pure rapeseed oil, color-coded based on the respective correlation coefficient (Pearson's r).**

Furthermore, correlations of the cooking mass spectra from this study with mass spectra of different aerosol types from previous studies were calculated (Fig. S2). The latter, obtained through PMF analysis of field measurement data, were taken from the AMS spectra database (Ulbrich et al., 2022) and averaged for the respective aerosol type (see Table S3 for list of used mass spectra).

225 The highest similarity of mass spectra related to oil- or fat- containing dishes was observed with the average COA mass spectrum ($r = 0.92 - 0.98$); therefore, we assume that also during field measurements the detected cooking-related emissions mostly consisted of vaporized and re-condensed oil. Furthermore, a strong correlation was observed between the mass spectra from the steak charcoal grilling experiment with the one of HOA, presumably due to the contribution of charcoal combustion to the overall emissions in this case.

230 3.1.2 Characteristics of mass spectra from cooking emissions

The main characteristics of the mass spectra from the cooking experiments agree with those of previous studies (Allan et al., 2010; Mohr et al., 2009; Mohr et al., 2012), exemplarily shown in Fig. S3 for the “frying bratwurst” experiment. The highest signal intensities were found at m/z 41 and 55, except for the boiled dish experiments. These signals are due to emissions of unsaturated hydrocarbons, presumably unsaturated fatty acids (He et al., 2010; Mohr et al., 2009). The most prominent ion series in the mass spectra are $C_nH_{2n+1}^+$ and $C_mH_{2m+1}CO^+$ (m/z 29, 43, 57, 71, ...), and $C_nH_{2n-1}^+$ and $C_mH_{2m-1}CO^+$ (m/z 41, 55, 69, 83, ...) from alkanes, alkenes, and oxygenated substances like acids, especially fatty acids. In addition, the ion series $C_nH_{2n-3}^+$ (m/z 67, 81, 95, 107, ...) and $C_6H_5C_nH_{2n}^+$ (m/z 77, 91, 105) indicate the presence of cycloalkanes and aromatic hydrocarbons (Alfarra et al., 2004; He et al., 2010; McLafferty and Turecek, 1993; Mohr et al., 2009).



240 A well-known indication for COA is a high ratio of m/z 55 to m/z 57, typically above two (Mohr et al., 2012; Sun et al., 2011; Xu et al., 2020). For the presented experiments, the observed ratio was 2.3 – 4.5, except for the boiled potatoes and the steaks grilled with charcoal with 1.3 and 1.7, presumably due to the fact that the respective emissions are not dominated by vaporized oil.

245 A comparison of the mass spectra with those of other typical aerosol types from the AMS spectra data base (Ulbrich et al., 2022) indicates that a ratio of m/z 67 to m/z 69 above 1 might be another potential COA marker. This ratio for HOA, BBOA, LVOOA, and SVOOA is ranging from 0.63 to 0.88 (Table S4). For the cooking experiments, the ratio was in the range of 1.1 – 1.6, again excluding the boiled potatoes and the steaks over charcoal grilling experiments with 0.81 and 0.7, respectively. The ratio for COA obtained from previous PMF analyses of ambient measurements is 1.2 ± 0.1 , while from direct measurements of cooking aerosols differing results were obtained. For emissions from Chinese cooking, heating sunflower, soy, corn, and rapeseed oil, and frying sausages and French fries with rapeseed and sunflower oil, the ratio was above 1 (Faber et al., 2013; He et al., 2010; Liu et al., 2017a; Liu et al., 2017b; Xu et al., 2020), while Allan et al. (2010) and Zhang et al. (2021) measured ratios below 1 from heating or cooking with rapeseed, sunflower, peanut, and corn oil; further it was below or close to 1 for barbecue emissions, frying meat, heating olive and palm oil, and lard (Kaltsonoudis et al., 2017; Liu et al., 2018; Xu et al., 2020).

250 Considering these studies, we conclude that the ratio of m/z 67 to m/z 69 in the mass spectra is dependent on the fatty acid composition and the fraction of polyunsaturated fatty acids in the measured aerosol. For saturated and monounsaturated fatty acids the ion series $C_nH_{2n-1}^+$ and $C_mH_{2m-1}CO^+$ (m/z 41, 55, 69, 83, ...) are more prominent, while for polyunsaturated fatty acids the ion series $C_nH_{2n-3}^+$ (m/z 67, 81, 95, 107, ...) is dominant (Christie, 2022; Hallgren et al., 1959). For oils from rapeseed, sunflower, and corn the fraction of polyunsaturated fatty acids is above 25% and the ratio of m/z 67 to m/z 69 mainly above 1. For oils with lower fractions of polyunsaturated fatty acids, like palm or olive oil, and animal fats, like lard, the ratio is below 1. Thus, the ratio of m/z 67 to m/z 69 might be an indicator for the composition of the oil used for cooking.

260 Emissions from biomass burning are mostly identified by the high signal intensity at m/z 60 and 73 which is due to the fragments $C_2H_4O_2^+$ and $C_3H_5O_2^+$ of levoglucosan generated by pyrolysis of cellulose (Schneider et al., 2006). During the laboratory cooking experiments, also elevated signal intensities for these ions were observed, however less intense than for biomass burning aerosols. These elevated signal intensities were also measured for emissions from pure heated rapeseed oil and also observed in reference mass spectra of the fatty acids oleic, stearic, and palmitic acid (AMS spectra database, Ulbrich et al., 2022), and therefore in these cases likely originate from fatty acids rather than levoglucosan, i.e. the ion structure contains a carboxyl group rather than a diol (Fachinger et al., 2017), leading to a different fragmentation pattern. A possibility to differentiate between biomass burning and cooking emissions therefore might be the ratio of m/z 60 to 73. The ratio for pure levoglucosan and BBOA are 3.7 and 1.5, respectively, while the ratios from the cooking experiments, excluding the boiled dishes due to low organic concentrations and high uncertainty, ambient COA, and fatty acids are at most 1.1 (Table 3). Similar observations were reported by Xu et al. (2020) who measured a ratio of ~ 2 for BBOA and around 1 for COA.

270



Table 3: Ratio of signal intensities at m/z 60 and 73 from mass spectra of different compounds and aerosol types. For BBOA, COA, and the cooking experiments the average and standard deviation was calculated from the available data. All mass spectra except for the cooking experiments were obtained from the AMS spectra database (Ulbrich et al., 2022).

| Ratio of signal intensities at m/z 60 and 73 | |
|--|-----------------|
| BBOA-related | |
| Levogluconan | 3.71 |
| BBOA | 1.47 ± 0.53 |
| COA-related | |
| Oleic acid | 0.81 |
| Stearic acid | 0.87 |
| Palmitic acid | 0.89 |
| COA | 1.10 ± 0.13 |
| Cooking experiments ^a | 0.90 ± 0.08 |
| Rapeseed oil | 0.95 |

275 ^aexcluding boiled dishes (low organic concentrations)

3.1.3 Discrimination of different aerosol types based on markers in their mass spectra

Ambient aerosol is usually a mixture of various aerosols of different types due to the contribution by different aerosol sources and aging processes in the atmosphere. To identify individual aerosol types and their contribution to the total aerosol, PMF is applied to the mass spectra of the measured organic aerosol fraction and the obtained factors are attributed to various aerosol types using different indicators and through comparison to other available data. For this study, a new type of diagram was applied to verify whether known and new indicators in the mass spectra are suitable to reliably differentiate between different aerosol types and to check whether PMF worked well for separating different aerosol contributions.

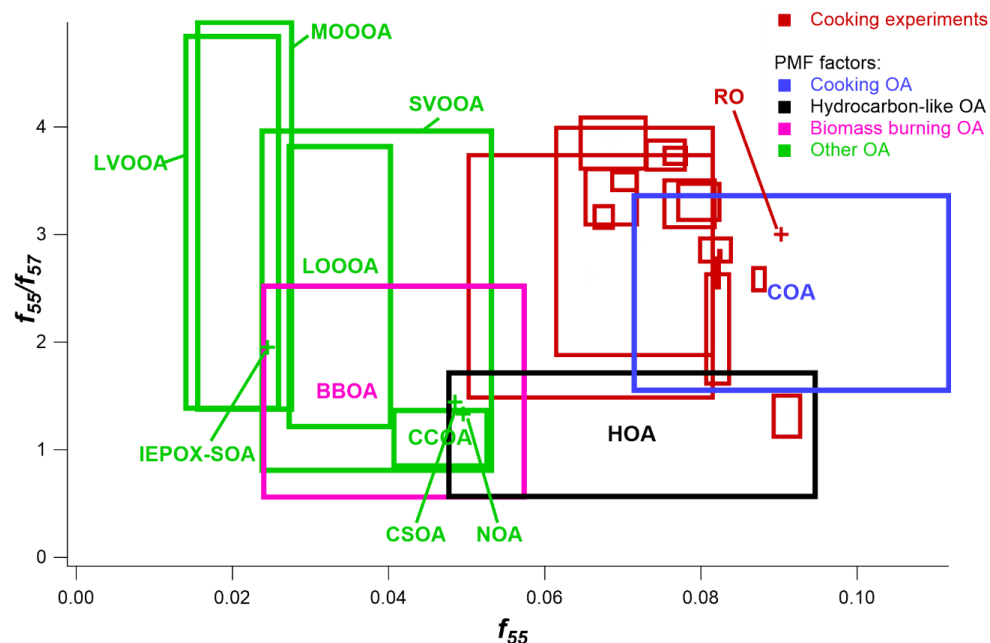
In these “rectangle plots”, the values of two indicators for all available aerosol types are plotted against each other in an xy-diagram. The standard deviation or uncertainty for each indicator of a certain aerosol type is reflected in x- and y-direction by a box to show the variability of the mass spectra for this aerosol type. The different aerosol types are well separated with a selected combination of indicators if there is no overlap of boxes. Indicators for individual aerosol types might be the fraction of the signal intensity at a single m/z from the total organic signal, e.g. f_{44} for the signal fraction at m/z 44, a combination of such fractions, e.g. f_{55}/f_{57} , or organic aerosol elemental ratios, like O/C and H/C .

For the cooking experiments, the respective values were calculated as average from the three repetitions, while for the individual reference aerosol types, available mass spectra from the AMS spectra database (Ulbrich et al., 2022) were averaged. The corresponding standard deviation is shown as box in both cases; if only one reference mass spectrum or one repetition was available (e.g., rapeseed oil, RO), only a marker is shown in the rectangle plot. The experiments with the boiled dishes were excluded from this analysis due to very low organic concentrations and resulting high uncertainties.

Plotting the two known COA markers, f_{55} and f_{55}/f_{57} , together in such a rectangle plot (Fig. 3) shows that the mass spectra of ambient COA and from the cooking experiments are well separated from those of other aerosol types with this selection of markers. The values for COA and the cooking experiments are in the top right corner with high f_{55} (> 0.06) and f_{55}/f_{57} (> 2) values. Though COA and HOA mass spectra are often similar, using both markers in combination they are well separated from each other, except for the experiment steaks grilled with charcoal which is located within the HOA box. The values of f_{55} for the cooking experiments are slightly lower than those from ambient COA while the f_{55}/f_{57} values are similar for both. This could either be due to the difference between ambient and laboratory aerosol, as ambient aerosol can chemically change in the atmosphere, or because PMF



is not able to separate the different aerosol types completely. The f_{55}/f_{57} versus f_{55} rectangle plot also shows that e.g. BBOA is not well separated from CCOA, CSOA and several OOA aerosol types, based on this combination of COA markers.



305 **Figure 3:** “Rectangle plot” of f_{55}/f_{57} combined with f_{55} for the cooking experiments and various organic aerosol types from ambient measurements. The acronyms for the different aerosol types are listed in Table 2; RO stands for rapeseed oil.

To determine whether the ratio f_{67}/f_{69} is suitable as COA marker, these ratios were plotted together with f_{55} in another “rectangle plot” (Fig. 4). Although the laboratory results and ambient COA are well separated from most other aerosol types, there is an overlap with HOA for two of the laboratory experiments. Therefore, we conclude that the ratio f_{67}/f_{69} might be a marker for COA similar as the ratio f_{55}/f_{57} , but the influence of the fatty acid composition of the emitted oil or fat needs to be considered (see Sect.

310 3.1.2). Therefore, the ratio of f_{67}/f_{69} should only be used as additional marker for COA.

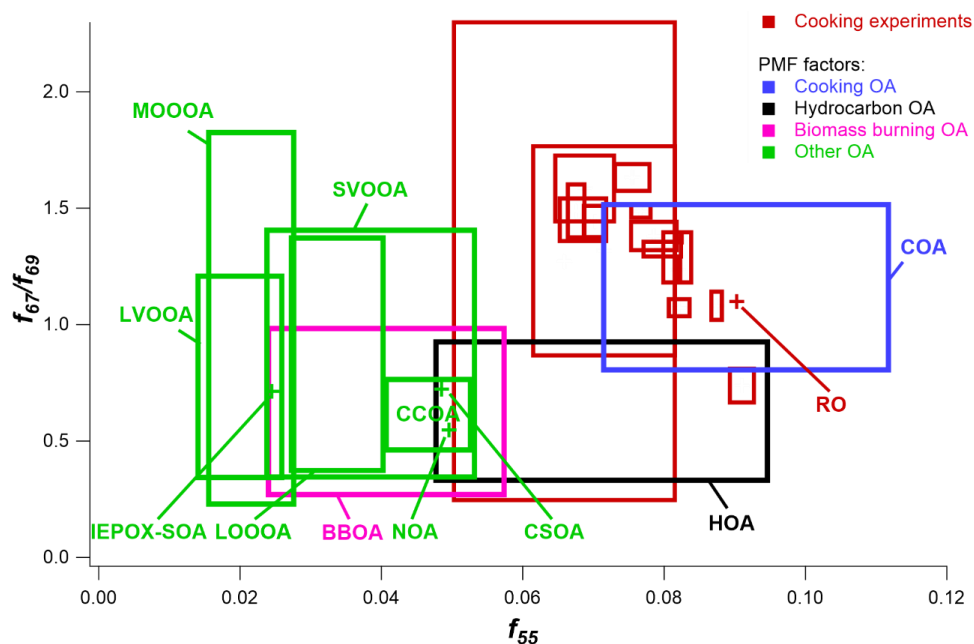


Figure 4: “Rectangle plot” of f_{67}/f_{69} combined with f_{55} for the cooking experiments and various organic aerosol types from ambient measurements. The acronyms for the different aerosol types are listed in Table 2; RO stands for rapeseed oil.

3.1.4 Relative ionization efficiency of cooking-related organic aerosol

315 The quantification of the aerosol species measured with the AMS is based on Eq. (2) (Canagaratna et al., 2007)

$$C_S = \frac{10^{12} MW_{NO_3}}{CE_S RIE_S IE_{NO_3} Q_{AMS} N_A} \sum_{all\ i} I_{S,i} \quad (2)$$

converting the ion rates of species S , $I_{S,i}$, summed over all i m/z , to mass concentrations C_S , with MW_{NO_3} the molecular weight of nitrate (in $g\ mol^{-1}$), Q_{AMS} the volumetric inlet flow rate (in $cm^3\ s^{-1}$), N_A Avogadro’s number and 10^{12} a unit conversion factor to $\mu g\ m^{-3}$. The remaining (unitless) factors in Eq. (2) are from calibrations or based on assumptions. The collection efficiency CE_S for the species S gives the ratio of particle mass measured by the AMS to the particle mass introduced to the inlet. It is mainly
 320 influenced by the particle phase, solid or liquid. The typical value for ambient aerosol is 0.5 accounting for mainly solid particles, a fraction of which bounces off the vaporizer without being vaporized. For particles from the presented cooking experiments, a CE value of 1 was chosen assuming that the emitted aerosol mostly consisted of liquid oil droplets (see Sect. 3.1.1) which do not bounce.

The ionization efficiency of nitrate IE_{NO_3} , determined in a calibration, is used as a basis to calculate the ionization efficiencies for
 325 other species, using the relative ionization efficiency of species S (RIE_S) relative to IE_{NO_3} . The default value for RIE_{Org} is 1.4 based on multiple laboratory experiments with various types of organic species (Canagaratna et al., 2007). As concentrations of COA measured with the AMS in previous studies were found to be higher compared to those from parallel measurements with other instruments, the RIE_{COA} is assumed to be larger than 1.4 (Katz et al., 2021; Reyes-Villegas et al., 2018; Yin et al., 2015).

In this work, RIE_{COA} was determined through comparison of the PM_{10} mass concentration determined from the FMPS and OPC
 330 measurements (PM_{10}) to the total AMS and black carbon mass concentration ($PM_{10,AMS+BC}$), measured in parallel. The oven and boiling experiments were excluded from this analysis due to almost exclusively low measured organic mass concentrations



($< 1 \mu\text{g m}^{-3}$). The density for the fine particles used to calculate PM_1 from the particle volume was in the range of $0.91 - 1.03 \text{ g cm}^{-3}$ (Table S5), determined individually for each dish (see Sect. S1). These values are in good agreement with the densities for cooking emissions found by Katz et al. (2021) ($0.95 - 1.0 \text{ g cm}^{-3}$), and, considering their uncertainty of 15%, also with that of rapeseed oil (0.91 g cm^{-3}), in agreement with our assumption that the particulate emissions from the cooking experiments consisted mainly of oil (see Sect. 3.1.1).

The measured PM_1 consisted mostly of organics (see Sect. 3.1.1; contribution of BC was negligible); consequently, as expected, $\text{PM}_{1,\text{AMS+BC}}$ was higher for most cooking experiments compared to PM_1 when using the default $\text{RIE}_{\text{Org}} = 1.4$. To determine RIE_{COA} for the individual experiments (or, more specifically, the product of RIE_{COA} and CE; we assume $\text{CE} = 1$), the $\text{PM}_{1,\text{AMS+BC}}$ time series was correlated with the one of PM_1 for each experiment separately and the RIE_{COA} was adjusted to obtain a slope of 1 for the correlation. For the grilling experiments, the RIE values were determined separately for the experimental phases “grilling” and “grill warm-up” with the latter ones not considered as RIE_{COA} . The resulting RIE_{COA} values for the cooking experiments were in the range of $1.53 - 2.52$ and thus frequently significantly above the default value of 1.4 (Fig. 5 and Table S5). The uncertainty for the determined RIE_{COA} value was estimated to be 38%, based on the method of Katz et al. (2021) with uncertainty propagation (see Sect. S3).

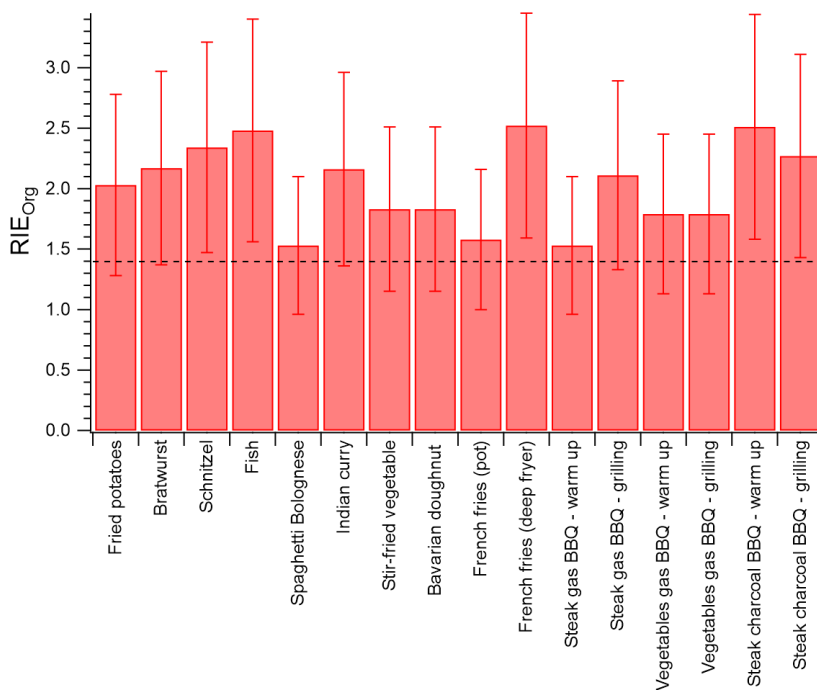


Figure 5: RIE_{COA} obtained for the different cooking experiments. The default RIE_{Org} of 1.4 is shown as dashed line.

In previous AMS studies of cooking-related emissions, the determined RIE_{COA} was also above 1.4. Reyes-Villegas et al. (2018) determined RIE values of $1.56 - 3.06$ for cooking emissions from different types of dishes through comparison of the measured concentrations ($\text{CE} = 1$) with SMPS (scanning mobility particle sizer) size distribution measurements ($d_p = 18 - 514 \text{ nm}$), comparable to our results. In contrast, from indoor aerosol measurements during cooking events, Katz et al. (2021) determined considerably higher RIE_{COA} values of $4.26 - 6.50$ with $\text{CE} = 1$, also through comparison with SMPS data ($d_p = 4 - 532 \text{ nm}$). A possible explanation for the larger values from Katz et al. (2021) could be that the RIE_{COA} depends on the fatty acid composition



355 of the oil droplets. For oleic acid, the main fatty acid of rapeseed oil which was used in the present study and the one of Reyes-Villegas et al. (2018), Katz et al. (2021) obtained an RIE value of 3.18 ± 0.95 , similar to the value of 3.0 measured by Xu et al. (2018), while for linoleic acid, the main component of soy oil, which Katz et al. (2021) used for their cooking experiments, an RIE value of 5.77 ± 1.73 was found.

Summarizing the results from the current and previous studies, we recommend for measurements close to cooking emission sources an RIE_{COA} larger than 1.4 for the COA fraction of the measured organic aerosol. Depending on the cooking oil, which presumably has a strong influence on the RIE_{COA} value, we suggest for soy oil-based cooking an average RIE_{COA} of 5.16 ± 0.77 (average of all measurements with standard deviation), based on the measurements by Katz et al. (2021), while for rapeseed oil-based cooking we recommend an average RIE_{COA} of 2.17 ± 0.48 (average of averages from both studies and standard error) based on the presented measurements of this study and the ones by Reyes-Villegas et al. (2018). The individual values used for this estimate are listed in Table S5.

3.2 Emission dynamics related to temperature and cooking activities

To study the emission dynamics during cooking as a consequence of different activities, the concentration time series determined for all dishes and for all measured variables were inspected in combination with the webcam recordings. For six emission variables increases and changes over the preparation time were identified: particle number concentration of smaller and larger particles measured by the CPC (PNC, $d_p > 5$ nm) and OPC (PNC_{d>250 nm}), PM concentration (PM₁, PM_{2.5}, PM₁₀), BC, PAH, and organics mass concentrations (shown exemplarily for the experiment “frying bratwurst” in Fig. S4). From these six, PNC_{d>250 nm}, organics and PM mass concentrations are all associated with the total emitted particle mass and therefore show similar emission dynamics. No increase above the detection limit was observed for the measured trace gas concentrations, except for NO_x during the grilling experiments and SO₂ during the charcoal grilling experiment.

375 For the six variables, two kinds of systematic changes were observed. Firstly, the measured concentrations for these variables increased over the preparation period, along with an increase of the food and cookware temperature, as deduced from repeated temperature measurements. The emission concentrations usually started to increase only after a certain heating or cooking period, probably when the used oil and food reached a certain temperature. Also, during inactivity of sufficiently long times, i.e. more than approximately 30 – 60 s, the PNC_{d>250 nm} and organics mass concentration increased as certain locations of the food reached sufficiently high temperatures. Such increased particle mass and number emissions with higher temperature were also observed in previous studies, e.g. by Buonanno et al. (2009), Amouei Torkmahalleh et al. (2012), and Zhang et al. (2010).

Reason for this progressive increase of concentrations is presumably the increasing vaporization of substances with rising temperatures. After emission, the vaporized substances cool down again, finally resulting in increased particle number and mass concentration due to nucleation and re-condensation. Accordingly, the emission concentrations decreased when the power of the stove was turned down.

385 An increase of BC and PAH mass concentrations was observed only for cooking methods operating at high temperatures like grilling or in the final phase of preparing stir-fried dishes. PAHs are formed at high temperature, especially above 400 °C, and due to incomplete combustion like during grilling, where BC is formed as well (Jägerstad and Skog, 2005; Lijinsky, 1991; Omidvarborna et al., 2015). The described dependence of the measured concentrations on temperature is shown schematically in Fig. 6.

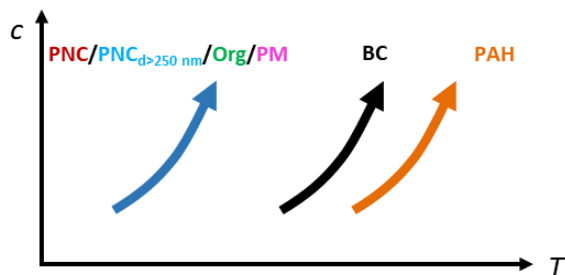
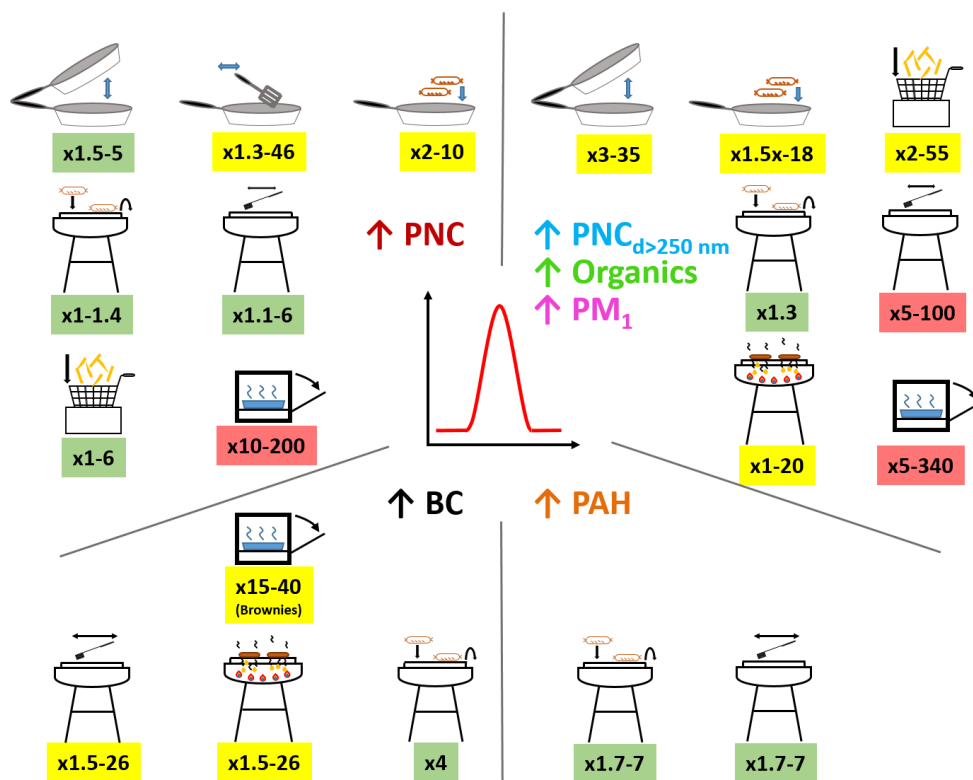


Figure 6: Schematic diagram of the temperature (T) dependence of the emission concentrations (c) of six relevant species.

The second systematic observation are short-time concentration changes associated with different activities during cooking, e.g. tilting the pan or flipping the food, which have not been studied in such detail so far. The activities leading to these short-time changes are schematically shown in Fig. 7 (symbols explained in Fig. S5), grouped by emission variables, with the increase factors by which the concentrations change from right before the increase up to the corresponding maximum concentration. The factors are color-coded, in green for relative increases below one order of magnitude, in yellow for increases above one order of magnitude and in red for increases above two orders of magnitude.

The emission concentrations rise briefly when hot material of the cooked food is brought to the surface by stirring or similar activities, facilitating vaporization. This leads to increased particle formation and growth through condensation of these substances. Furthermore, contact of cold, water-containing food with strongly heated surfaces, such as the pan, grill or hot oil, leads to rapid vaporization of oil, various other substances, and, above all, water, which can cause bubbling of oil. The associated enhancement of the oil surface leads to increased vaporization of oil and mechanical formation of larger particles due to bursting of oil bubbles. These processes rapidly decrease as the hot surface cools down. Similarly, short-term increases in concentration occur when droplets or components of the grilled food, as well as residues from cleaning the grate, fall onto hot surfaces, such as the charcoal, and quickly vaporize or burn. Due to the high temperatures at these locations, also transient concentration increases of BC and PAH are generated. The strongest increases in the emission concentrations for almost all variables were observed when the oven was opened during baking, presumably due to the low concentrations before the oven was opened and the sudden release of emissions which had accumulated within the oven.

410



415 **Figure 7: Schematic diagram of short-time concentration increases for the different variables due to various activities during preparation of the dishes (see Fig. S5 for the meaning of the symbols). PM_1 is shown representatively for PM. The range of factors by which the concentrations typically increase are shown as numbers and color-coded, in green for small, in yellow for medium and in red for high concentration increases.**

3.3 Influence of preparation method and cooking activities on the particle size distribution

The averaged particle number and volume size distributions of the emitted aerosols were similar for dishes with the same preparation method in terms of position and intensity of the particle mode. An overview of the mode diameters for the aerosols emitted during preparation of different dishes, grouped by the preparation method or dish type, is shown in Table 4. The average standard deviation of the mode diameters from the three repetitions was 5 nm for the particle number size distribution and 25 nm for the particle volume size distribution. Therefore, the observed differences between the distributions for the different preparation methods were partially significant.

425 The particle number distribution for most dishes was dominated by Aitken mode particles. The mode diameters ($d_{p,N}$) varied, depending on the preparation method, between 20 – 50 nm (Fig. S6). During the warm up phase of the grilling experiments, the size distribution was broader and plateau-like, presumably due to a combination of different particle generation processes like combustion of leftovers from the grid and incomplete combustion of the charcoal, but also dominated by Aitken mode particles (10 – 30 nm).

430 The average volume size distributions showed more variability for different preparation methods (Fig. S7). The distributions were mostly bimodal with an Aitken or accumulation mode and a coarse mode. During baking and grilling with gas the mode diameter of the fine particles was in the Aitken mode range ($d_{p,V} = 50 – 70$ nm) while during frying and grilling with charcoal the distribution was dominated by accumulation mode particles (200 – 300 nm). The coarse mode diameter was in the range of 2 – 3 μ m.



Table 4: Range of mode diameters from the averaged particle number and volume size distributions for particles emitted from the cooking of different dishes, sorted by mode diameter ($dN/d\log d_p$).

| Preparation method/ dish type | Dishes | Mode diameter $dN/d\log d_p$ ($d_{p,N}$) | Mode diameter $dV/d\log d_p$ ($d_{p,V}$) |
|----------------------------------|---|--|---|
| Grill warm up (gas, charcoal) | | 20 – 30 nm | Gas: 50 – 60 nm, 2.5 – 3 μm Charcoal: 300 nm, 720 nm, 2.2 μm |
| Deep-frying in pot | French fries, Bavarian doughnut | 20 – 30 nm | 275 – 280 nm, 2 μm |
| Stir-frying with sauce | Spaghetti Bolognese, stir-fried vegetables, Indian curry | 20 – 35 nm | 205 – 220 nm, 2 – 3 μm |
| Grilling with gas | Vegetable skewers, steak | 30 – 35 nm | 60 – 70 nm, 2 – 5 μm |
| Baking | Baked potatoes, pizza, brownies | 30 – 35 nm | 45 – 70 nm, 2 – 3 μm |
| Stir-frying | Fried potatoes, bratwurst, schnitzel, fish | 40 – 50 nm | 205 – 220 nm, 2 – 3 μm |
| Deep-frying in deep fryer | French fries | 50 nm | 205 nm, 2 – 3 μm |
| Grilling with charcoal | Steak | 50 nm | 205 nm, 600 nm, 2.2 μm |
| Boiling | Boiled potatoes, rice, noodles | No clear result due to small concentrations | 300 – 465 nm |

435

Presumably, the observed mode diameter of the emitted fine (i.e. submicron) aerosol is mostly influenced by the temperature of the prepared food and cookware. With higher temperature more oil and other substances can vaporize, leading to stronger particle growth and consequently larger particles. For example, particles from stir-fried dishes were larger ($d_{p,N} = 40 - 50$ nm) than from stir-fried dishes with sauce (20 – 35 nm) as the addition of the sauce cooled down the food and pan and the sauce effectively covered the hottest part of the system, the base of the pan. Furthermore, the available amount of material which can vaporize influences the particle growth. For example, during frying, compared to baking, more oil is available which can vaporize, leading to larger particles. During grilling with charcoal, compared to gas, the particles were larger as the incomplete combustion of charcoal generates smoke and, due to the higher temperature, additional substances can vaporize, also from the charcoal itself.

440

The coarse mode particles are generated by mechanical processes, presumably from oil bubble bursting. During grilling with charcoal, the combustion of the charcoal also leads to the emission of coarse particles. The particles emitted from the boiled dishes are presumably initially coarse particles from water bubble bursting with droplets containing dissolved salt and other food components which shrink due to the low relative humidity to accumulation mode particles.

445

In accordance with our measurements, similar dependencies for the mode diameter of the temperature and available amount of material which can vaporize were observed in previous studies. With increasing cooking temperatures Amouei Torkmahalleh et al. (2012), Buonanno et al. (2009), and Zhang et al. (2010) measured particle size distributions with larger mode diameters. Furthermore, Buonanno et al. (2009) observed for emissions from grilling (without oil on electric or gas grill) of fatty foods, like cheese, bacon, and sausage larger number mode diameters ($d_{p,N} = 40 - 50$ nm) compared to those from cooking vegetables ($d_{p,N} = 30$ nm) showing that the availability of easily vaporizable substances, here fat, leads to larger particles.

450

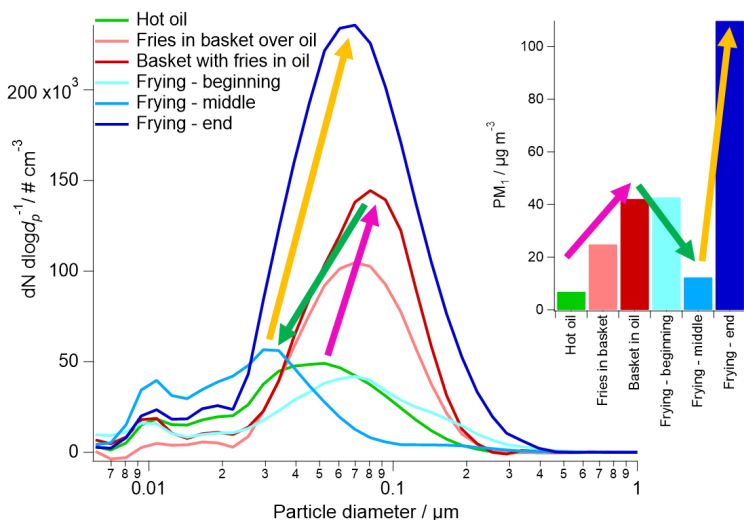
Apart from the preparation method, which is mainly characterized by the cooking temperature and availability of water, oil, or fat, individual activities during the cooking also influence the particle size distribution of the emitted aerosol. Such influences are shown in Fig. 8 using the example of deep-frying French fries in the deep fryer, showing the number size distributions (15 - 30 s

455



time periods, averaged over all repetitions) of emissions during different activities or preparation phases. Included are the corresponding PM₁ mass concentrations for the same periods; colored arrows illustrate the temporal changes.

In the beginning, the particle number concentration, size and mass concentration increase as the frozen fries are placed in the basket above the oil and then submerged into the oil (pink arrow). When the fries are put into the basket, the oil starts to bubble as small parts of the fries and ice crystals drop into the hot oil and the water vaporizes immediately. The bubbling increases when the fries are submerged into the oil as more water rapidly vaporizes. The bubbles lead to a larger oil surface, enhancing the vaporization of oil and therefore the particle formation and growth. As a consequence of the frozen fries in the oil, the oil cools down and less oil vaporizes and consequently the particle number concentration, size and mass concentration decrease (green arrow). As the oil slowly heats up again towards the end of the cooking process all variables increase again due to increased oil vaporization (yellow arrow).



470 **Figure 8: Average number size distribution and PM₁ mass concentration for six different cooking activities / periods during the preparation of French fries in the deep fryer. The arrows illustrate the temporal trends.**

The presented example illustrates the main parameters which influence the particle emissions: 1. the temperature of the prepared food and cookware, 2. the oil surface, and 3. the available amount of vaporable material, as also observed for the particle number concentration and mass concentration for various variables (see Sect. 3.2). Similar dependencies were also observed during the preparation of other dishes (Table 5). Usually the mode diameter increased over the preparation period, as observed e.g. during the heating of the oven and grilling with charcoal. Presumably, the temperature increase of the food and the cookware led to stronger vaporization of oil and other substances. Also, various activities during the preparation of the food resulted in transient changes of the size of the emitted particles analogous to the changes of the emission intensity, as presented in Sect. 3.2. In addition, when the grid of the grill was cleaned with a brush, the particle size increased, presumably because leftovers fell off grid onto the charcoal and burned or vaporized. A similar process was observed when steaks were cut on the grill and the meat juice drops vaporized off the hot grid or charcoal, leading to larger particles as well.

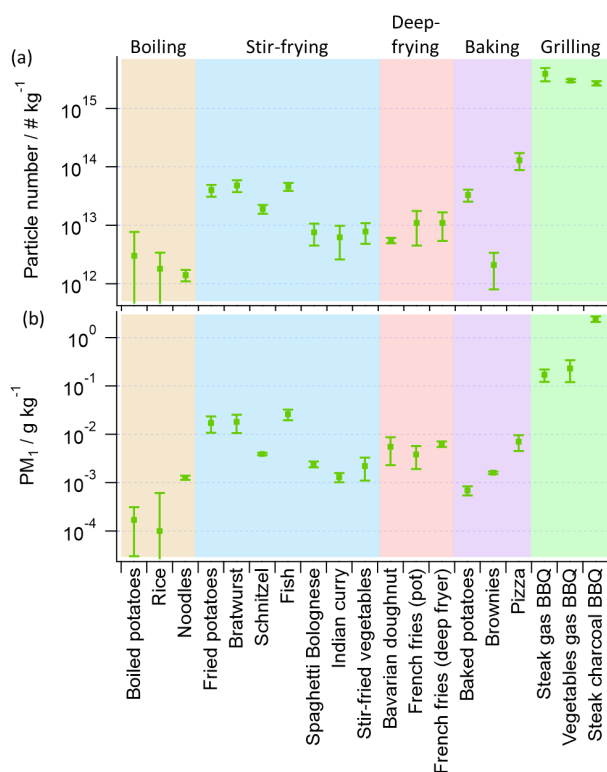


Table 5: Overview of the particle mode diameter changes due to individual activities.

| Process/activity | Mode diameter dN/dlogd _p | Reason |
|--------------------------------|-------------------------------------|---|
| Grilling on charcoal | 35 nm → 170 nm | Increase of temperature over time |
| Stir-frying | 30 nm → 60 nm | Increase of temperature over time |
| Heating of oven | 17 nm → 40 nm | Increase of temperature over time |
| Cleaning the grid of the grill | Increase by 5 – 10 nm | Food leftovers from the grid vaporized on hot surface |
| Cutting steaks on grill | Increase by 5 – 10 nm | Meat juice vaporized from hot surface |

3.4 Quantification of cooking emissions: Emission factors

485 To be able to quantitatively estimate emissions from cooking activities and their impact on air quality based on the mass of prepared food, emission factors (amount of emitted substance per kg of prepared food) were calculated for all dishes from this study and for all relevant variables (Table S6). The PN (particle number, as measured by the CPC) and PM₁ emission factors are shown exemplarily in Fig. 9 for all dishes, grouped by the respective preparation method. For other mass-based variables, e.g. organics, the general trends are similar to those of PM₁, which are described in the following.



490

Figure 9: Emission factors for (a) PN and (b) PM₁ for all dishes, with standard deviation from the three repetitions as error bars. The values are grouped by the preparation methods, highlighted with different colors.

For dishes with the same preparation method the emission factors are similar and at most one order of magnitude apart from each other. The highest PN emission factors were observed for the grilling experiments with up to $4 \cdot 10^{15} \text{ kg}^{-1}$ while the emission factors

495 for the oil-based or fat-containing dishes, including the preparation methods stir-frying, deep-frying, and baking, are substantially



smaller, ranging from $2.1 \cdot 10^{12} - 1.3 \cdot 10^{14} \text{ kg}^{-1}$. The smallest emission factors were observed for boiled dishes with values up to $3 \cdot 10^{12} \text{ kg}^{-1}$.

A similar trend was observed for PM_1 with highest emission factors for the grilling experiments ($0.2 - 2.4 \text{ g kg}^{-1}$) and one to two orders of magnitude smaller emission factors for stir-fried, deep-fried and baked dishes ($7 \cdot 10^{-4} - 0.026 \text{ g kg}^{-1}$). Again, the smallest emission factors were found for boiled dishes ($1 \cdot 10^{-4} - 1.3 \cdot 10^{-3} \text{ g kg}^{-1}$).

The $\text{PN}_{d>250 \text{ nm}}$ (number of particles measured by the OPC, i.e. with $d_p > 250 \text{ nm}$) emission factors range from $5 \cdot 10^7 - 2 \cdot 10^{10} \text{ kg}^{-1}$ for boiled and baked dishes, from more than $2 \cdot 10^{10} - 9 \cdot 10^{11} \text{ kg}^{-1}$ for stir-fried, deep-fried, and gas-grilled dishes, and up to $2 \cdot 10^{13} \text{ kg}^{-1}$ for the charcoal-grilled dish. BC and PAH emissions were only observed for dishes where cooking temperatures were sufficiently high for their formation, e.g. the grilling and stir-frying experiments ($18 - 28,000 \mu\text{g kg}^{-1}$ and $3 - 208 \mu\text{g kg}^{-1}$, respectively). Sulfate was only observed for dishes containing onions and grilled dishes ($6 - 354 \mu\text{g kg}^{-1}$). The emission factors for all variables are listed in Table S6.

Generally, the trends in the observed emission factors for the different preparation methods were similar for the different measured variables. For mass-based or -related variables (PM_1 , organics, PAH, BC, and $\text{PN}_{d>250 \text{ nm}}$) the emission factors from the charcoal grilling experiment are usually one order of magnitude higher compared to those of the gas grilling experiments. The incomplete combustion of the charcoal leads to the additional emission of smoke which includes larger particles and in total higher emitted mass. The combustion of charcoal during the warm up of the grill contributes already 34 – 52% of the total emissions for the whole cooking experiment, depending on the variable (PN, NO_x , organics: 34 – 40 %; PAH, $\text{PM}_{1/2.5/10}$, $\text{PN}_{d>250 \text{ nm}}$: 40 – 50 %; BC: 52 %). The emissions from grilling, compared to other preparation methods, are one to two orders of magnitude higher presumably due to burning of food leftovers from the grid and due to the higher temperatures leading to more vaporization of substances and hence increased particle formation and growth due to re-condensation.

The emission factors for the stir-fried, deep-fried, and baked dishes were similar to each other as in these cases the emissions are mostly due to vaporization and re-condensation of oil and other substances as well as mechanical processes like vaporization of water leading to oil bubbling and splashing. The lowest emissions were observed for boiled dishes which was the only applied preparation method without any oil or fatty food involved. For this preparation method, the only source for particles is bubble bursting leading to droplets which contain dissolved salt or other components.

Oil based cooking (e.g. deep-frying and stir-frying) leading to higher particle number concentrations compared to water-based cooking (boiling and steaming) was also observed by See and Balasubramanian (2006), Wu et al. (2012), and Zhang et al. (2010). Similar observations were made for the emitted particle mass (Alves et al., 2014; See and Balasubramanian, 2006) and PAH emissions (Chen et al., 2007; Zhao et al., 2019).

For comparison with the results from previous studies, PN and $\text{PM}_{2.5}$ emission rates (Table 6) were calculated for 1 kg of cooked food and 60 min preparation time (assuming that the food preparation takes one hour) for different preparation methods. The emission rates determined from our experiments were mostly comparable to those obtained from previous studies (He et al., 2004; Liao et al., 2006) or agreed with them within an order of magnitude (Lee et al., 2001; Nasir and Colbeck, 2013). In contrast, up to two orders of magnitude higher emission rates were reported by Buonanno et al. (2009) for PN and by Olson and Burke (2006) for $\text{PM}_{2.5}$ emissions.



Table 6: PN and PM_{2.5} emission rates for 1 kg of cooked food per hour preparation time, for different preparation methods. Comparison of our results with those of previous studies.

| | PN / kg ⁻¹ h ⁻¹ | PM _{2.5} / mg kg ⁻¹ h ⁻¹ |
|--------------------------|---|---|
| Stir-frying | | |
| This work | 5.2 · 10 ¹³ | 23 |
| Buonanno et al. (2011) | 4.5 · 10 ¹⁵ – 5.4 · 10 ¹⁵ | |
| Nasir and Colbeck (2013) | 8 · 10 ¹² | 78 |
| He et al. (2004) | 1.5 · 10 ¹³ | |
| Baking | | |
| This work | 8.6 · 10 ¹³ | 5 |
| Nasir and Colbeck (2013) | 2.6 · 10 ¹³ | 45 |
| He et al. (2004) | 1.2 · 10 ¹³ | |
| Olson and Burke (2006) | | 600 |
| Grilling | | |
| This work | | 280 – 2700 |
| Olson and Burke (2006) | | 10380 |
| Deep-frying | | |
| This work | | 10 |
| Liao et al. (2006) | | 3.2 – 8 |
| Lee et al. (2001) | | 70 |
| Olson and Burke (2006) | | 3600 |

535 In the case of the study by Buonanno et al. (2011), these differences may be caused by different measurement conditions, as the
emissions in that study were measured in a closed kitchen with mechanical ventilation, at a distance of 2 m from the stove and not
by capturing all emissions as in our study. In the case of the study by Olson and Burke (2006), who performed measurements with
body-worn instruments to assess personal exposure, the massively larger emission rates they found compared to our and previous
studies were presumably due to a combination of reasons. Firstly, the high relative humidity during cooking led to larger particles
and consequently an overdetermination of particle concentrations due to increased light scattering in the nephelometers, which
were used in their study to infer PM_{2.5}. In addition, the authors assumed that the emissions would be diluted equally in the whole
apartment volume; however, as stated in their manuscript, inhomogeneous distribution of the emissions caused differences in the
inferred emission rates depending on the measurement location (i.e. kitchen vs. living room). Finally, for their calculations of the
emission rates they considered only the peak concentrations during cooking, while in the present study the whole cooking period
was considered.

Overall, the comparison of emission rate measurements shows that the obtained emission rates are dependent not only on the
cooking conditions themselves, but also on the measurement (dilution) conditions and the method to calculate the emission factors
or rates. This complicates the comparison of different studies.

To obtain an idea about the relevance of the emissions from cooking activities in relation to those from other emission sources,
emissions from the various preparation methods were compared with emissions from traffic, biomass burning, burning of candles,
and smoking. To this end, we calculated the emissions from these sources for activities over a period of one hour each, i.e. for the
one-time preparation of a dish (“cooking”), for driving a car over a distance of 100 km (“traffic”), for smoking two cigarettes
(“smoking”), and for biomass burning-based heating a room of 50 m² (“biomass burning”) or burning a candle (“candle burning”)



for one hour. The emission factors for the various activities were taken from the literature, as summarized in Table S7. As these activities are chosen partially arbitrary, this comparison only serves as a rough classification of cooking emissions compared to those of other emission sources.

The calculated emissions for the dishes with the same preparation method were averaged for four variables: PN, PM₁, BC, and PAH (Fig. 10 and Fig. S8), and their standard deviation is used as uncertainty. For the emissions from other sources, the ranges of emissions calculated from the emission factors found in the literature are presented as bars to reflect the variability of emission levels.

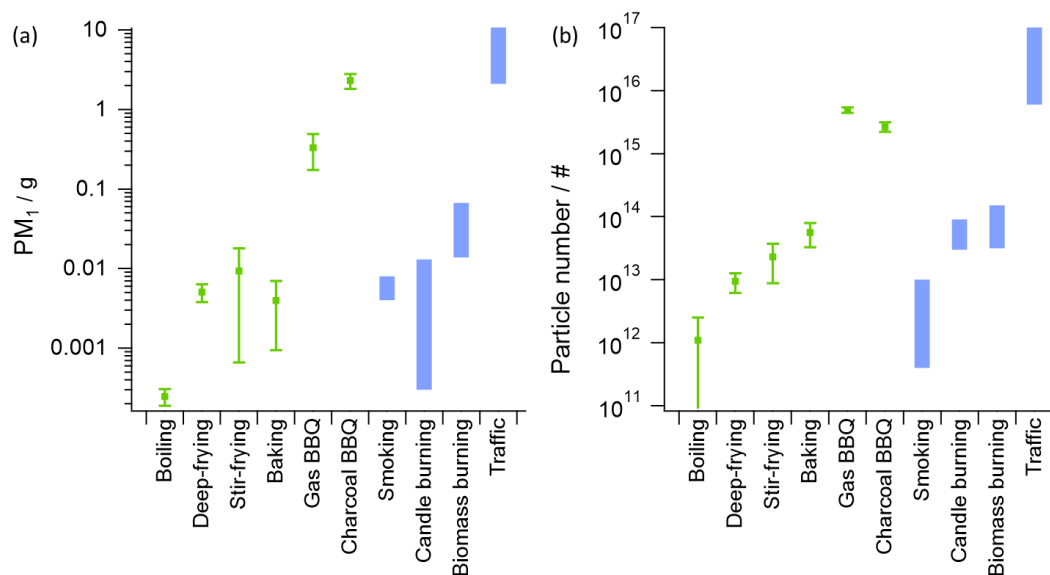


Figure 10: Total emissions of (a) PM₁ mass and (b) particle number for cooking one dish, averaged for the different preparation types with the standard deviation as error bars, and comparison with emissions from various other activities during one hour, shown as bars indicating the variability found in the literature.

For the mass-based variables (PM₁, BC, PAH) the highest cooking emissions which were from charcoal grilling are in the same range as those observed from traffic, indicating the potential for a significant local impact of grilling on air quality. This assumption is supported by a study of Kaltsonoudis et al. (2017), which shows that during a Greek holiday when traditionally meat is grilled everywhere in the city the contribution of COA reached up to 85% of the measured organic aerosol.

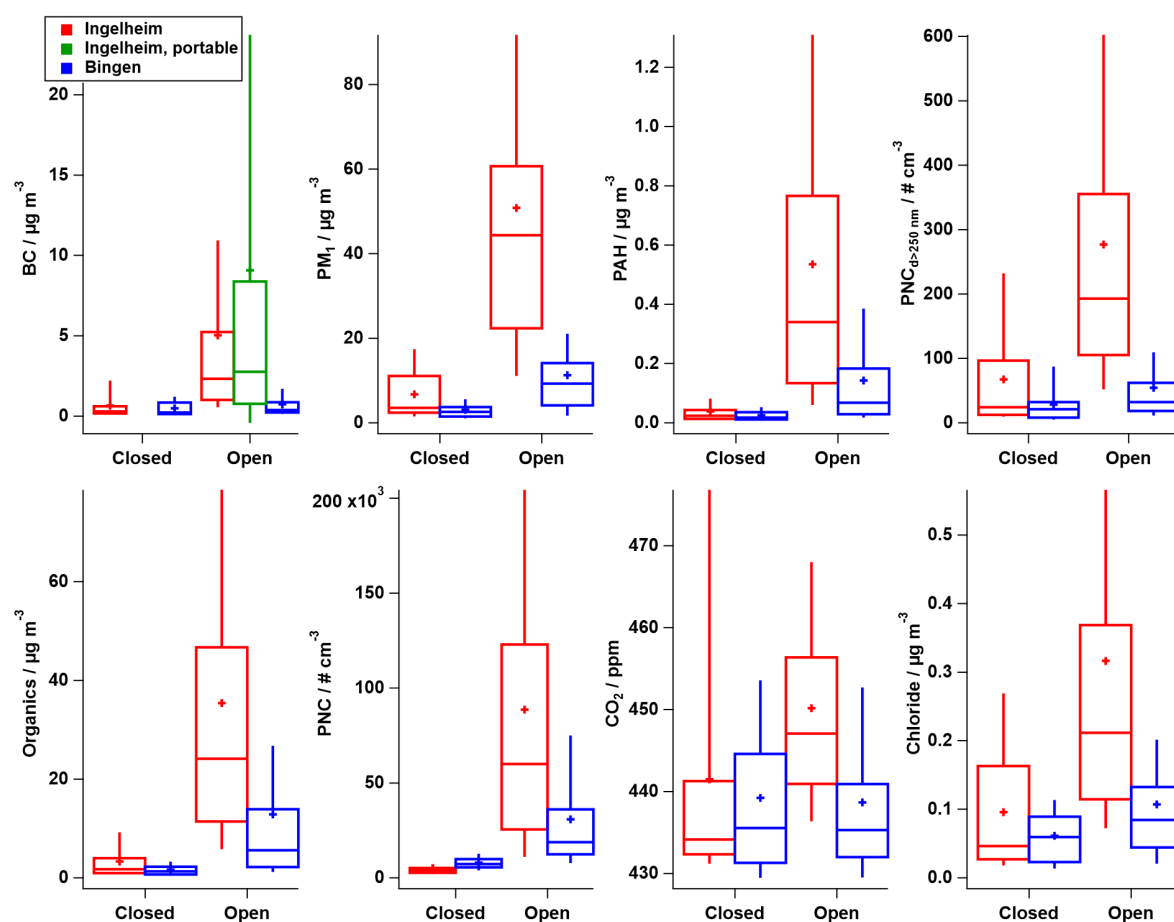
Stir-frying, deep-frying and baking, all oil-based preparation methods, show emissions of similar order of magnitude to each other, typically on the lower end of emissions from biomass burning-based room heating, and on the upper end of emissions from candle burning and cigarette smoking. This finding is consistent with observations from ambient measurements, which show that COA can easily make up similar proportions of total organics as traffic- and biomass burning-related organic aerosols, especially in urban environments (e.g., Mohr et al., 2012; Struckmeier et al., 2016). In indoor environments, cooking is one of the major emission sources leading to high emissions of fine particulate matter, number and mass wise, even exceeding the emissions due to light smoking (Abdullahi et al., 2013; Zhou et al., 2016; He et al., 2004).

Boiling, on the other hand, causes much smaller emissions, which are at the lower end or even below those of smoking and candle burning. Unlike oil-based preparation methods, boiling therefore will usually have no strong contribution to the total ambient aerosol load, which is in line with the conclusion that ambient COA consists mainly of externally mixed (Freutel et al., 2013) oil droplets (Allan et al., 2010).



3.5 Ambient measurements at two Christmas markets

At both Christmas markets, substantial aerosol concentration increases were measured during the opening hours compared to the background (i.e., the hours when the markets were closed) for the same six species which were also relevant during the laboratory measurements: PNC and PNC_{d>250 nm}, PM, BC, PAH, and organics mass concentrations (Fig. S9 and Fig. S10). Additionally, CO₂ and particulate chloride concentrations increased, especially at the market in Ingelheim, presumably due to burning of wood at the market (Fachinger et al., 2018; Levin et al., 2010; Williams et al., 2012). A summary of measured concentrations (represented in box plots) for time periods inside and outside the opening hours is shown in Fig. 11, which illustrates the increase of concentrations due to the Christmas market emissions.



590 **Figure 11:** Pollutant concentrations measured during (open) and outside (closed) the opening hours for the Christmas markets in Ingelheim (red and green) and Bingen (blue). For each variable, the average concentration is shown as cross, the 25th and 75th percentiles as box, with the median as horizontal bar, and the 10th and 90th percentiles as whiskers.

In Ingelheim, the median PNC and the organics, PM₁ and PAH mass concentrations were larger during the opening hours by more than one order of magnitude compared to the background period. The median PNC_{d>250 nm}, BC, and particulate chloride mass concentrations were enhanced by a factor of 4 – 8. The median CO₂ volume mixing ratio was larger by 13 ppm. In Bingen, the median concentration enhancements due to the Christmas market emissions were smaller: for organics, PM₁, and PAH mass concentrations by a factor of 3.5 – 4.5, for the other variables by a factor of 1.5 – 2.5, except for CO₂, which did not show an increase during the opening hours.



The different concentration levels between both locations during the opening hours are presumably due to two reasons. First, in
600 Ingelheim the measurement location was very close (few meters) to the food stands, while in Bingen the distance to the next food
stand was about 25 m. Second, the Christmas market in Ingelheim was larger with more visitors and food stands which stood more
densely. Generally, the measurements show that emissions from a Christmas market might lead to substantial pollutant
concentration enhancements at a local level.

In Ingelheim, the BC mass concentrations were additionally measured with a portable aethalometer (Fig. 11, green box plot for
605 BC) while repeatedly walking across the Christmas market during the opening hours to estimate the personal exposure of market
visitors. The median value measured during these mobile measurements across the market was similar to the median value from
the stationary measurements directly downwind the market. This indicates that the measured concentrations at a single location at
the downwind edge are representative for the overall market. At the same time, the average concentration measured with the
portable instrument ($9.1 \mu\text{g m}^{-3}$) was almost twice as high as the average of the stationary measurements ($5.0 \mu\text{g m}^{-3}$). Thus, visitors
610 of the market can be exposed to much higher transient BC concentrations, presumably when they walk close by fire places or other
strong sources, increasing their personal exposure.

3.5.1 PMF analysis of the AMS organics data

For detailed information about the contribution of different aerosol types, the AMS organics mass spectra were analyzed using
positive matrix factorization (PMF), separately for both Christmas markets. For both markets, BBOA, COA, and OOA (which is
615 usually associated with aged background aerosol), were identified as aerosol types from the most reasonable PMF solution (Figs.
S11 and S12). The challenge during this analysis was that two emission sources, cooking and biomass burning, were close to each
other with similar activity times, while a requirement for the PMF algorithm to separate different types of aerosols is a characteristic
temporal variation, different for each aerosol type. This resulted in an incomplete separation of the OOA factor for the
measurements in Ingelheim with considerable OOA concentration increases during the opening hours of the market, while for this
620 background-related aerosol type rather constant concentrations independent of the opening times are expected (as seen in Bingen).
The mass spectra of COA, BBOA, and OOA are similar for both locations and exhibit the typical markers for the respective aerosol
types. In the mass spectra of OOA the most intense signal is at m/z 44 (CO_2^+), originating from thermal decomposition of oxidized
organic compounds (Ng et al., 2010). BBOA could be identified by the elevated signal intensities at m/z 60 and 73, whose ratio of
2.6 at both markets points to levoglucosan (see Sect. 3.1.2), which is a result of the pyrolysis of cellulose (Schneider et al., 2006).
625 In the COA mass spectra, the highest signal intensities are at m/z 41 and 55 and the signal ratio of m/z 55 and 57 is 2.6, which is
consistent with results from previous studies (Mohr et al., 2012; Sun et al., 2011; Xu et al., 2020) and our laboratory studies
(Sect. 3.1.2). The correlation with corresponding reference mass spectra (averaged from the available mass spectra from the AMS
database, see Table S3) supported the assignment of the identified factors, with correlation coefficients of 0.93 and 0.97 for COA,
0.98 and 0.95 for OOA, and 0.83 and 0.77 for BBOA, for Ingelheim and Bingen, respectively.
630 The COA and BBOA concentrations were significantly enhanced during the opening hours while the OOA concentrations
remained almost constant (OOA for Ingelheim not regarded here due to incomplete separation). The average concentrations of
COA (CE = 1; RIE = 2.27; see Sect. 3.5.2) were $3.5/0.14 \mu\text{g m}^{-3}$ and $2.5/0.05 \mu\text{g m}^{-3}$ and of BBOA (CE = 0.5; RIE = 1.4) $17.1/0.54$
 $\mu\text{g m}^{-3}$ and $2.4/0.21 \mu\text{g m}^{-3}$ during/outside the opening hours for Ingelheim and Bingen, respectively. In Bingen the OOA
concentration (CE = 0.5; RIE = 1.4) were mostly below $2 \mu\text{g m}^{-3}$ over the whole measurement period suggesting that this PMF
635 factor can be attributed to the background aerosol. The observed stepwise changes of the OOA concentration (Fig. S11) were due
to wind direction changes. The fraction of OOA at both Christmas markets during the opening hours was similar with 15 %
and 17 %, while BBOA amounts to 71 % and 40 % and COA to 14 % and 43 % for Ingelheim and Bingen, respectively. The higher



BBOA fraction in Ingelheim might be due to a second wood fire barrel at 25 m distance to MoLa on two afternoons and a flame-grilled salmon stand with an open wood fire within the food stands circle where MoLa was located.

640 3.5.2 Validation of laboratory measurements using the Christmas market data

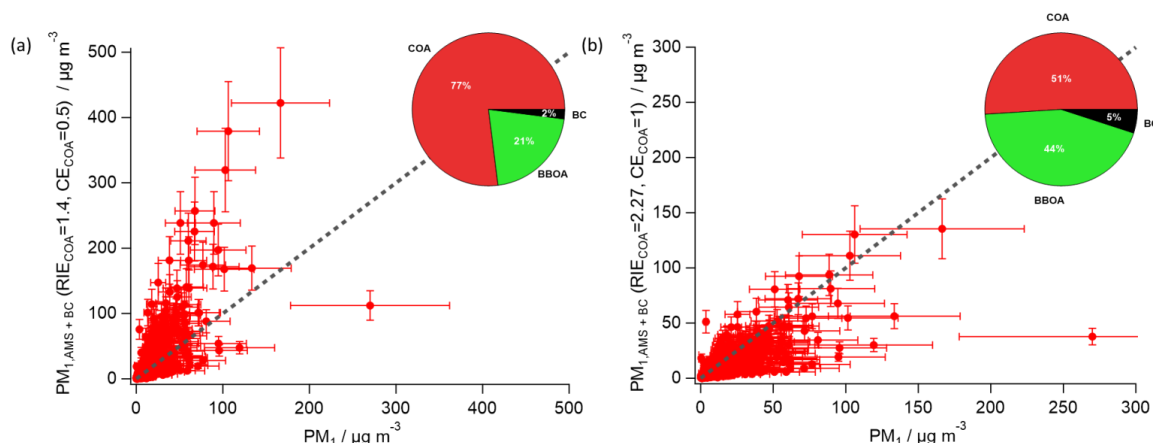
To assess whether the results from the laboratory experiments are also applicable to ambient measurements, we used the Christmas market data to verify different aspects of our results. Due to the higher fraction of COA measured during the Christmas market opening hours in Bingen (43 %) compared to Ingelheim (14 %) the analysis was only performed with the data set collected in Bingen.

645 The dishes prepared at the Christmas market which were also studied in the laboratory are bratwurst frying, deep-frying French fries (in a deep fryer), and steaks grilled on a gas grill. A linear correlation of the average COA mass spectrum from the PMF analysis of the Christmas market data with the mass spectra of the above mentioned three dishes showed very high similarity between the spectra (Pearson's $r = 0.99$), as did the correlation with the one of rapeseed oil ($r = 0.98$) and oleic acid ($r = 0.93$). The ratio of f_{67}/f_{69} for this COA mass spectrum was 1.4, similar to the ratios of previously measured ambient COA (1.2 ± 0.1) and
650 the laboratory measurements (1.1 – 1.6), supporting our suggestion of f_{67}/f_{69} as additional COA marker (see Sect. 3.1.2).

To verify whether the densities for the organic fraction derived from the cooking emission experiments can be applied to ambient measurements, the densities for the three Christmas market-related dishes as well as for the COA PMF factor from the measurements at the market were calculated based on the formula of Kuwata et al. (2012). The density of COA with 0.94 g cm^{-3} is in agreement with the densities for the three dishes ($0.94 - 0.98 \text{ g cm}^{-3}$, Table S5). This finding along with the high mass spectral
655 similarity discussed above suggests that the observed ambient COA mostly consisted of vaporized and re-condensed oil.

In order to validate whether the RIE_{COA} values determined from laboratory measurements are applicable to ambient measurements of cooking-related aerosols, PM_{10} (from FMPS and OPC measurements, Sect. S1) was compared to PM_{10} calculated from BC and AMS species ($\text{PM}_{10, \text{AMS+BC}}$) for two different value sets of RIE_{COA} and CE_{COA} : i) the default AMS values, i.e. $\text{RIE}_{\text{COA}} = 1.4$ and $\text{CE}_{\text{COA}} = 0.5$ (Fig. 12a); and ii) average values derived from the laboratory measurements of the three Christmas market-related
660 dishes ($\text{RIE}_{\text{COA}} = 2.27$ and $\text{CE}_{\text{COA}} = 1$; Fig. 12b). Additionally, the fractions of the different aerosol species of the Christmas market PM_{10} emissions (after background subtraction) are shown in Fig. 12 as pie charts which were calculated by applying for COA the respective RIE and CE values. In both cases, default RIE and CE values were used for the other AMS species including BBOA and OOA (i.e., assuming externally mixed COA; Freutel et al., 2013). According to Fig. 12a, $\text{PM}_{10, \text{AMS+BC}}$ seems to be overestimated when using the default values, while with RIE_{COA} and CE_{COA} taken from the laboratory results the PM_{10} values align reasonably
665 well with the one-to-one line (Fig. 12b), suggesting a better mass closure, though no definitive answer can be given due to the low correlation coefficient in both cases ($r = 0.56$ and 0.58 with the default and laboratory values, respectively). The pie charts highlight the effect of the different RIE and CE values on the calculated fraction of COA of the emitted Christmas market PM_{10} . Using the default values, the COA fraction would be 26% larger compared to that when using the laboratory values, showing the importance of choosing correct RIE and CE values for COA.

670 Generally, the result of this comparison is in agreement with those of previous ambient measurements of cooking emissions which also suggest a higher RIE_{COA} value than the default RIE_{Org} of 1.4 (Katz et al., 2021; Reyes-Villegas et al., 2018).



675 **Figure 12: Comparison of measured $PM_{1,AMS+BC}$ with PM_1 with (a) $RIE_{COA} = 1.4$, $CE_{COA} = 0.5$ and (b) $RIE_{COA} = 2.27$, $CE_{COA} = 1$ for the COA fraction. The 1:1 line serves as guidance. The pie charts show the calculated PM_1 composition of the Christmas market emissions (i.e., only for opening times, after background subtraction).**

Based on the results of the laboratory experiments as well as those of previous studies, no strong contribution of BC was expected from cooking emissions (Zhang et al., 2010; Zhao et al., 2007), and the observed BC was assumed to originate mainly from biomass burning. Indeed, the ratio of BBOA ($RIE = 1.4$ and $CE = 0.5$) to BC mass concentrations on average was 3.3 during the Christmas market opening times, which is well within the range of 1.7 – 33 observed for open biomass burning (Reid et al., 2005) and close to the ratios of 4.0 and 3.16 measured for mainly domestic heating in urban environments by Crippa et al. (2013) and Elser et al. (2016).

The applicability of the laboratory emission factors (see Sect. 3.4) to ambient measurements was verified by testing whether they can reproduce the concentrations measured during the Christmas market in a simple model. For this purpose, the emission factors for dishes which were prepared at the Christmas market were used (bratwurst frying, deep-frying French fries in the deep fryer and steaks from the gas grill) for the variables PN, PM_1 , and organics. Gas grilling rather than charcoal grilling emission factors were used here since PMF likely apportions part of the charcoal grilling to the biomass burning factor, causing an underestimate of the respective COA emissions.

The emissions per hour (EM) needed to generate the measured concentrations were calculated using the average concentration during the opening hours ($\overline{c_{CM}}$) minus the average background concentration ($\overline{c_{BG}}$) and the volumetric flow rate Q_{CM} with which the emissions were diluted (Eq. (3)). The volumetric flow rate Q_{CM} was estimated based on the average wind speed ($1.15 m s^{-1}$, mostly from the west), the height of the houses (8 m) surrounding the square up to which we assumed the emissions would be diluted, and the width of the street that runs from west to east transporting most of the air mass, resulting in $Q_{CM} = 5 \cdot 10^5 m^3 h^{-1}$ ($138 m^3 s^{-1}$). Finally, using the emission factors EF from the laboratory experiments, we calculated which amount of food (m) would be needed to be cooked per hour in order to generate the calculated emissions per hour (Eq. (4)).

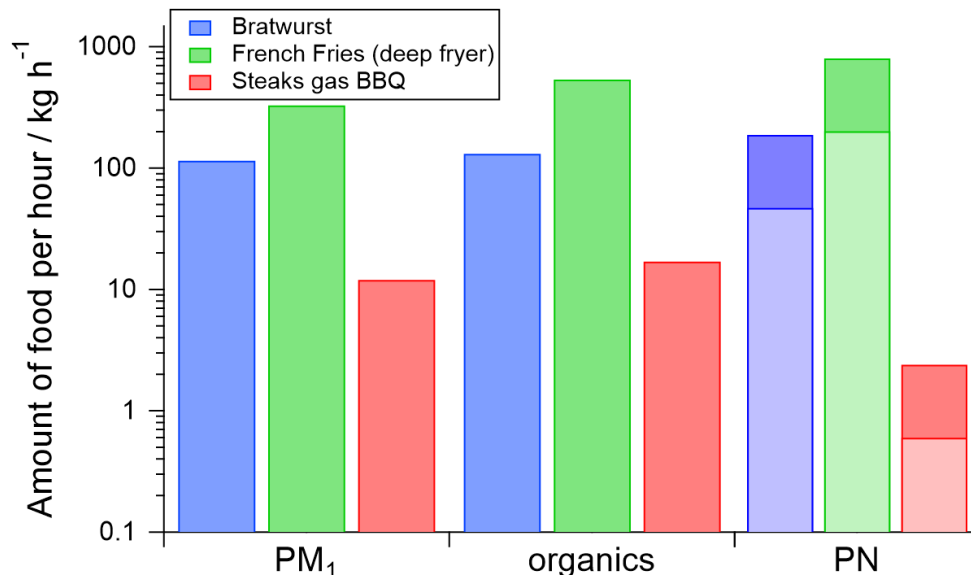
$$EM = (\overline{c_{CM}} - \overline{c_{BG}}) \cdot Q_{CM} \quad (3)$$

$$m = \frac{EM}{EF} \quad (4)$$

As the emission factors were determined from cooking activities, we considered only the COA-related fraction of the measured Christmas market emissions for the mass-based variables PM_1 and organic mass concentration. The COA concentration was



calculated using $RIE_{COA} = 2.27$ and $CE_{COA} = 1$ and considering only the emissions of the Christmas market (background subtracted). For PM_{10} the fraction that is related to COA amounts to 51% (Fig. 12b), and for the total measured AMS organics to 54%. As it is not possible to determine the COA-related fraction for PN based on the results for PM_{10} , we estimated that the COA fraction for PN would be somewhere between 20% and 80% and performed the calculations for these two extreme scenarios. Figure 13 shows for the three chosen variables the amount of food which would be needed to be cooked of the respective single dishes per hour in order to account for the observed emissions. For the mass-based variables, the calculated masses for steaks were 12 – 17 $kg\ h^{-1}$ and for bratwurst and French fries at least one order of magnitude higher with 115 – 538 $kg\ h^{-1}$. For PN, the calculated food amount for the chosen COA fraction range of 20% to 80% was similar as for the mass-based variables with 0.6 – 2.4 $kg\ h^{-1}$ of steaks and 47 – 803 $kg\ h^{-1}$ of bratwurst and French fries. These calculated masses of food prepared per hour are all in a realistic order of magnitude (especially for the steak dish), suggesting that the laboratory-derived emission factors for PN, PM_{10} and organics are applicable to ambient measurements within an acceptable range of uncertainty.



710

Figure 13: Amount of food which needs to be prepared per hour to generate the same concentrations (after background subtraction) as measured at the Christmas market in Bingen, calculated based on the emissions factors for three different dishes and on the local aerosol transport conditions. For each variable, the respective COA fraction was calculated with $RIE_{COA} = 2.27$ and $CE = 1$ and for PN a COA fraction range of 20% (light bar) to 80% (dark bar) was assumed.

715 4 Conclusion

In a comprehensive laboratory study, various aspects of cooking-related emissions were studied in real time with multiple instruments, including the chemical composition of PM_{10} and particle size distributions as well as emission dynamics and the quantification of emissions through calculation of emission factors. In addition, the influence of cooking activities on the ambient aerosol was investigated at two German Christmas markets.

720 From the laboratory experiments, it was found that measured particle number concentrations as well as several mass-based variables (PM_{10} , BC, PAH, organics) were strongly affected by the cooking activities. Measurements with the AMS indicate that the PM_{10} fraction of the measured emissions was mostly composed of oil as shown through comparison of the mass spectra of the



measured emissions with the one of rapeseed oil, the used cooking oil. Therefore, we assume that particle formation and growth is mainly the result of oil vaporization and re-condensation.

725 Through comparison of the AMS-measured organics mass concentrations with the mass concentration derived from size distributions, we found that higher values for the RIE_{COA} (1.53 – 2.52) compared to the default value of 1.4 are required for correct determination of mass concentrations of cooking-related organic aerosols. These results confirm and extend the findings of previous studies. As a conclusion, we recommend using different RIE_{COA} values depending on the cooking oil since it has an influence on the RIE_{COA} : for cooking with rapeseed oil an RIE_{COA} of 2.17 ± 0.48 based on this study and the one by Reyes-Villegas et al. (2018), and for soy oil-based cooking an RIE_{COA} of 5.16 ± 0.77 based on the measurements by Katz et al. (2021).

730 Furthermore, to support the AMS data analysis of organic aerosol types, a new diagram type is presented that enables a simple and quick way to check whether PMF succeeded in separating different aerosol types using known markers and also to identify and validate new markers, e.g. for real-time identification of aerosol types. Using the data of multiple measurement campaigns, the variability of the mass spectra for individual aerosol types is accounted for and this provides the opportunity to evaluate how well the separation of aerosol types works, based on the selected markers. Here, we identified and evaluated the ratio $f_{67}/f_{69} > 1$ as additional COA marker. The presented examples show the importance of combining markers or indicators to achieve a robust separation from other aerosol types, like for COA $f_{55} (> 0.06)$ and $f_{55}/f_{57} (> 2)$ for separation especially from HOA.

The relevant parameters influencing the amount of cooking emissions are the cooking temperature, use of oil, ingredients, and activities during the cooking process. These are mostly dependent on the preparation method; hence we observed similar results for dishes with similar preparation methods. A change of concentrations of the relevant variables (PM, BC, PAH, organics) as well as of the particle size could be attributed to changes of the temperature of the food and cookware as well as different activities during the preparation. Due to rising temperature, more substances vaporize and condense leading to higher emissions as well as larger particles. The emission of BC and PAH was observed only at higher temperature, e.g. towards the end of preparation. Different activities lead to transient concentration and particle size changes as they 1. facilitate the vaporization of substances, e.g. through stirring or tilting the pan, 2. increase the amount of vaporizable material, e.g. by cleaning the grill grid, or 3. suddenly release accumulated emissions, e.g. by opening the oven.

745 The used ingredients themselves also have a strong influence on the aerosol composition. The emissions from boiled dishes differ from the emissions of other dishes mostly due to the broad absence of oil and fatty ingredients. Another example is the occurrence of sulfur-containing species in the emitted aerosol for dishes with fried onions.

750 For quantification of the emissions, emission factors were determined for all relevant variables individually for all dishes. The highest emissions were released from preparing dishes on a gas and a charcoal grill due to the highest cooking temperatures, burning of food leftovers from the grid, and, in the case of charcoal grilling, due to additional emissions from the charcoal burning itself. The emission levels from cooking stir-fried, deep-fried, and baked dishes were similar to each other as oil or fatty ingredients were used for all dishes. The preparation of boiled dishes resulted in the release of the lowest emissions as no oil was used, limiting the amount of vaporizable substances. Furthermore, a comparison to other relevant indoor and ambient emission sources showed that grilling one dish emits similar amounts of particles as driving 100 km by car and emissions from oil-based cooking, like frying, are of similar order of magnitude as such from domestic biomass burning over a comparable time interval.

755 The average PM_1 concentrations during the opening hours at a Christmas market were found to be as high as $51 \mu g m^{-3}$. Locally, visitors could be exposed to even higher concentrations as shown for BC concentrations measured with a portable aethalometer across the market, which were on average twice as high as those of the stationary measurements immediately downwind the market. Though this is not a 24 h average value, these elevated concentrations show that events like Christmas markets have a strong influence on local air quality.



This result together with those from the laboratory measurements show that cooking activities contribute substantially to indoor and ambient aerosol. The amount of emissions is mainly determined by the preparation method, with barbecues as especially strong
765 emission source.

Author contribution. JP and FD conceptualized the measurements. JP carried out the experiments, analyzed the MoLa data with
770 support from FF and prepared the paper with contributions from FD, FF und SB.

Competing interests. The authors declare that they have no conflict of interest.

Acknowledgements. We thank Thomas Böttger and the mechanical workshop for technical support. The authors thank David
775 Troglauer, Lasse Moormann, and Philipp Schuhmann for support during the laboratory measurements. We also thank the organizers of the Christmas markets for the possibility to perform our measurements. Furthermore, we acknowledge the Max Planck Institute for Chemistry for funding of this work.



References

- 780 Abbatt, J. P. D. and Wang, C.: The atmospheric chemistry of indoor environments, *Environmental Science: Processes & Impacts*, 22, 25–48, <https://doi.org/10.1039/c9em00386j>, 2020.
- Abdullahi, K. L., Delgado-Saborit, J. M., and Harrison, R. M.: Emissions and indoor concentrations of particulate matter and its specific chemical components from cooking: A review, *Atmospheric Environment*, 71, 260–294, <https://doi.org/10.1016/j.atmosenv.2013.01.061>, 2013.
- 785 Alfarrá, M. R., Coe, H., Allan, J. D., Bower, K. N., Boudries, H., Canagaratna, M. R., Jimenez, J. L., Jayne, J. T., Garforth, A. A., Li, S.-M., and Worsnop, D. R.: Characterization of urban and rural organic particulate in the Lower Fraser Valley using two Aerodyne Aerosol Mass Spectrometers, *Atmospheric Environment*, 38, 5745–5758, <https://doi.org/10.1016/j.atmosenv.2004.01.054>, 2004.
- Allan, J. D., Williams, P. I., Morgan, W. T., Martin, C. L., Flynn, M. J., Lee, J., Nemitz, E., Phillips, G. J., Gallagher, M. W., and
790 Coe, H.: Contributions from transport, solid fuel burning and cooking to primary organic aerosols in two UK cities, *Atmos. Chem. Phys.*, 10, 647–668, <https://doi.org/10.5194/acp-10-647-2010>, 2010.
- Alves, C. A., Duarte, M., Nunes, T., Moreira, R., and Rocha, S.: Carbonaceous particles emitted from cooking activities in Portugal, *Global NEST Journal*, 16, 411–419, <https://doi.org/10.30955/gnj.001313>, 2014.
- Alves, C. A., Evtyugina, M., Cerqueira, M., Nunes, T., Duarte, M., and Vicente, E.: Volatile organic compounds emitted by the
795 stacks of restaurants, *Air Quality, Atmosphere & Health*, 8, 401–412, <https://doi.org/10.1007/s11869-014-0310-7>, 2015.
- Amouei Torkmahalleh, M., Goldasteh, I., Zhao, Y., Udochu, N. M., Rossner, A., Hopke, P. K., and Ferro, A. R.: PM_{2.5} and ultrafine particles emitted during heating of commercial cooking oils, *Indoor Air*, 22, 483–491, <https://doi.org/10.1111/j.1600-0668.2012.00783.x>, 2012.
- Baron, P. A., Kulkarni, P., and Willeke, K. (Eds.): *Aerosol measurement: Principles, techniques, and applications*, 3rd ed.,
800 Engineering professional collection, John Wiley & Sons, Inc., New York, 883 pp., 2011.
- Boelens, M., Valois, P. J. de, Wobben, H. J., and van der Gen, A.: Volatile flavor compounds from onion, *J. Agric. Food Chem.*, 19, 984–991, <https://doi.org/10.1021/jf60177a031>, 1971.
- Buonanno, G., Johnson, G., Morawska, L., and Stabile, L.: Volatility Characterization of Cooking-Generated Aerosol Particles, *Aerosol Science and Technology*, 45, 1069–1077, <https://doi.org/10.1080/02786826.2011.580797>, 2011.
- 805 Buonanno, G., Morawska, L., and Stabile, L.: Particle emission factors during cooking activities, *Atmospheric Environment*, 43, 3235–3242, <https://doi.org/10.1016/j.atmosenv.2009.03.044>, 2009.
- Canagaratna, M. R., Jayne, J. T., Jimenez, J. L., Allan, J. D., Alfarrá, M. R., Zhang, Q., Onasch, T. B., Drewnick, F., Coe, H., Middlebrook, A., Delia, A., Williams, L. R., Trimborn, A. M., Northway, M. J., DeCarlo, P. F., Kolb, C. E., Davidovits, P., and Worsnop, D. R.: Chemical and microphysical characterization of ambient aerosols with the aerodyne aerosol mass
810 spectrometer, *Mass Spectrometry Reviews*, 26, 185–222, <https://doi.org/10.1002/mas.20115>, 2007.
- Chafe, Z. A., Brauer, M., Klimont, Z., van Dingenen, R., Mehta, S., Rao, S., Riahi, K., Dentener, F., and Smith, K. R.: Household cooking with solid fuels contributes to ambient PM_{2.5} air pollution and the burden of disease, *Environmental Health Perspectives*, 122, 1314–1320, <https://doi.org/10.1289/ehp.1206340>, 2014.
- Chen, Y., Ho, K. F., Ho, S. S. H., Ho, W. K., Lee, S. C., Yu, J. Z., and Sit, E. H. L.: Gaseous and particulate polycyclic aromatic hydrocarbons (PAHs) emissions from commercial restaurants in Hong Kong, *J. Environ. Monit.*, 9, 1402–1409, <https://doi.org/10.1039/b710259c>, 2007.
- 815 Cheng, S., Wang, G., Lang, J., Wen, W., Wang, X., and Yao, S.: Characterization of volatile organic compounds from different cooking emissions, *Atmospheric Environment*, 145, 299–307, <https://doi.org/10.1016/j.atmosenv.2016.09.037>, 2016.



- Christie, W. W.: The Lipid Web, https://www.lipidmaps.org/resources/lipidweb/lipidweb_html/index.html, last access: 18
820 September 2022, 2022.
- Crippa, M., DeCarlo, P. F., Slowik, J. G., Mohr, C., Heringa, M. F., Chirico, R., Poulain, L., Freutel, F., Sciare, J., Cozic, J., Di
Marco, C. F., Elsasser, M., Nicolas, J. B., Marchand, N., Abidi, E., Wiedensohler, A., Drewnick, F., Schneider, J.,
Borrmann, S., Nemitz, E., Zimmermann, R., Jaffrezo, J.-L., Prévôt, A. S. H., and Baltensperger, U.: Wintertime aerosol
825 chemical composition and source apportionment of the organic fraction in the metropolitan area of Paris, *Atmos. Chem.
Phys.*, 13, 961–981, <https://doi.org/10.5194/acp-13-961-2013>, 2013.
- Diffey, B. L.: An overview analysis of the time people spend outdoors, *The British journal of dermatology*, 164, 848–854,
<https://doi.org/10.1111/j.1365-2133.2010.10165.x>, 2011.
- Drewnick, F., Böttger, T., Weiden-Reinmüller, S.-L. v. d., Zorn, S. R., Klimach, T., Schneider, J., and Borrmann, S.: Design of a
mobile aerosol research laboratory and data processing tools for effective stationary and mobile field measurements, *Atmos.*
830 *Meas. Tech.*, 5, 1443–1457, <https://doi.org/10.5194/amt-5-1443-2012>, 2012.
- Elser, M., Huang, R.-J., Wolf, R., Slowik, J. G., Wang, Q., Canonaco, F., Li, G., Bozzetti, C., Daellenbach, K. R., Huang, Y.,
Zhang, R., Li, Z., Cao, J., Baltensperger, U., El-Haddad, I., and Prévôt, A. S. H.: New insights into PM_{2.5} chemical
composition and sources in two major cities in China during extreme haze events using aerosol mass spectrometry, *Atmos.*
Chem. Phys., 16, 3207–3225, <https://doi.org/10.5194/acp-16-3207-2016>, 2016.
- 835 Faber, P., Drewnick, F., Veres, P. R., Williams, J., and Borrmann, S.: Anthropogenic sources of aerosol particles in a football
stadium: Real-time characterization of emissions from cigarette smoking, cooking, hand flares, and color smoke bombs by
high-resolution aerosol mass spectrometry, *Atmospheric Environment*, 77, 1043–1051,
<https://doi.org/10.1016/j.atmosenv.2013.05.072>, 2013.
- Fachinger, F., Drewnick, F., Gieré, R., and Borrmann, S.: Communal biofuel burning for district heating: Emissions and
840 immissions from medium-sized (0.4 and 1.5 MW) facilities, *Atmospheric Environment*, 181, 177–185,
<https://doi.org/10.1016/j.atmosenv.2018.03.014>, 2018.
- Fachinger, J. R. W., Gallavardin, S. J., Helleis, F., Fachinger, F., Drewnick, F., and Borrmann, S.: The ion trap aerosol mass
spectrometer: field intercomparison with the ToF-AMS and the capability of differentiating organic compound classes via
MS-MS, *Atmos. Meas. Tech.*, 10, 1623–1637, <https://doi.org/10.5194/amt-10-1623-2017>, 2017.
- 845 Freutel, F., Schneider, J., Drewnick, F., Weiden-Reinmüller, S.-L. v. d., Crippa, M., Prévôt, A. S. H., Baltensperger, U., Poulain,
L., Wiedensohler, A., Sciare, J., Sarda-Estève, R., Burkhardt, J. F., Eckhardt, S., Stohl, A., Gros, V., Colomb, A., Michoud,
V., Doussin, J. F., Borbon, A., Haefelin, M., Morille, Y., Beekmann, M., and Borrmann, S.: Aerosol particle measurements
at three stationary sites in the megacity of Paris during summer 2009: meteorology and air mass origin dominate aerosol
particle composition and size distribution, *Atmos. Chem. Phys.*, 13, 933–959, <https://doi.org/10.5194/acp-13-933-2013>,
850 2013.
- Gao, J., Cao, C., Wang, L., Song, T., Zhou, X., Yang, J., and Zhang, X.: Determination of Size-Dependent Source Emission Rate
of Cooking-Generated Aerosol Particles at the Oil-Heating Stage in an Experimental Kitchen, *Aerosol Air Qual. Res.*, 13,
488–496, <https://doi.org/10.4209/aaqr.2012.09.0238>, 2013.
- Goldstein, A. H., Nazaroff, W. W., Weschler, C. J., and Williams, J.: How Do Indoor Environments Affect Air Pollution
855 Exposure?, *Environmental Science & Technology*, 55, 100–108, <https://doi.org/10.1021/acs.est.0c05727>, 2021.
- Hallgren, B., Ryhage, R., Stenhagen, E., Sömme, R., and Palmstierna, H.: The Mass Spectra of Methyl Oleate, Methyl Linoleate,
and Methyl Linolenate, *Acta Chem. Scand.*, 13, 845–847, <https://doi.org/10.3891/acta.chem.scand.13-0845>, 1959.



- He, C., Morawska, L., Hitchins, J., and Gilbert, D.: Contribution from indoor sources to particle number and mass concentrations in residential houses, *Atmospheric Environment*, 38, 3405–3415, <https://doi.org/10.1016/j.atmosenv.2004.03.027>, 2004.
- 860 He, L.-Y., Lin, Y., Huang, X.-F., Guo, S., Xue, L., Su, Q., Hu, M., Luan, S.-J., and Zhang, Y.-H.: Characterization of high-resolution aerosol mass spectra of primary organic aerosol emissions from Chinese cooking and biomass burning, *Atmos. Chem. Phys.*, 10, 11535–11543, <https://doi.org/10.5194/acp-10-11535-2010>, 2010.
- IPCC: *Climate Change 2021: The Physical Science Basis*, Cambridge University Press, Cambridge, New York, 2021.
- Jägerstad, M. and Skog, K.: Genotoxicity of heat-processed foods, *Mutation Research*, 574, 156–172, <https://doi.org/10.1016/j.mrfmmm.2005.01.030>, 2005.
- 865 Kaltonoudis, C., Kostenidou, E., Louvaris, E., Psichoudaki, M., Tsiligiannis, E., Florou, K., Liangou, A., and Pandis, S. N.: Characterization of fresh and aged organic aerosol emissions from meat charbroiling, *Atmos. Chem. Phys.*, 17, 7143–7155, <https://doi.org/10.5194/acp-17-7143-2017>, 2017.
- Katz, E. F., Guo, H., Campuzano-Jost, P., Day, D. A., Brown, W. L., Boedicker, E., Pothier, M., Lunderberg, D. M., Patel, S., 870 Patel, K., Hayes, P. L., Avery, A., Hildebrandt Ruiz, L., Goldstein, A. H., Vance, M. E., Farmer, D. K., Jimenez, J. L., and DeCarlo, P. F.: Quantification of cooking organic aerosol in the indoor environment using aerodyne aerosol mass spectrometers, *Aerosol Science and Technology*, 55, 1099–1114, <https://doi.org/10.1080/02786826.2021.1931013>, 2021.
- Klein, F., Platt, S. M., Farren, N. J., Detournay, A., Bruns, E. A., Bozzetti, C., Daellenbach, K. R., Kilic, D., Kumar, N. K., Pieber, S. M., Slowik, J. G., Temime-Roussel, B., Marchand, N., Hamilton, J. F., Baltensperger, U., Prévôt, A. S. H., and El 875 Haddad, I.: Characterization of Gas-Phase Organics Using Proton Transfer Reaction Time-of-Flight Mass Spectrometry: Cooking Emissions, *Environmental Science & Technology*, 50, 1243–1250, <https://doi.org/10.1021/acs.est.5b04618>, 2016.
- Kreyling, W. G., Semmler-Behnke, M., and Möller, W.: Health implications of nanoparticles, *J Nanopart Res*, 8, 543–562, <https://doi.org/10.1007/s11051-005-9068-z>, 2006.
- Kuwata, M., Zorn, S. R., and Martin, S. T.: Using elemental ratios to predict the density of organic material composed of carbon, 880 hydrogen, and oxygen, *Environmental Science & Technology*, 46, 787–794, <https://doi.org/10.1021/es202525q>, 2012.
- Lee, S. C., Li, W.-M., and Lo Yin Chan: Indoor air quality at restaurants with different styles of cooking in metropolitan Hong Kong, *Science of The Total Environment*, 279, 181–193, [https://doi.org/10.1016/S0048-9697\(01\)00765-3](https://doi.org/10.1016/S0048-9697(01)00765-3), 2001.
- Levin, E. J. T., McMeeking, G. R., Carrico, C. M., Mack, L. E., Kreidenweis, S. M., Wold, C. E., Moosmüller, H., Arnott, W. P., Hao, W. M., Collett, J. L., and Malm, W. C.: Biomass burning smoke aerosol properties measured during Fire Laboratory at 885 Missoula Experiments (FLAME), *J. Geophys. Res.*, 115, 1783, <https://doi.org/10.1029/2009jd013601>, 2010.
- Liao, C.-M., Chen, S.-C., Chen, J.-W., and Liang, H.-M.: Contributions of Chinese-style cooking and incense burning to personal exposure and residential PM concentrations in Taiwan region, *Science of The Total Environment*, 358, 72–84, <https://doi.org/10.1016/j.scitotenv.2005.03.026>, 2006.
- Lijinsky, W.: The formation and occurrence of polynuclear aromatic hydrocarbons associated with food, *Mutation Research/Genetic Toxicology*, 259, 251–261, [https://doi.org/10.1016/0165-1218\(91\)90121-2](https://doi.org/10.1016/0165-1218(91)90121-2), 1991.
- 890 Liu, T., Wang, Z., Huang, D. D., Wang, X., and Chan, C. K.: Significant Production of Secondary Organic Aerosol from Emissions of Heated Cooking Oils, *Environ. Sci. Technol. Lett.*, 5, 32–37, <https://doi.org/10.1021/acs.estlett.7b00530>, 2018.
- Liu, T., Li, Z., Chan, M., and Chan, C. K.: Formation of secondary organic aerosols from gas-phase emissions of heated cooking oils, *Atmos. Chem. Phys.*, 17, 7333–7344, <https://doi.org/10.5194/acp-17-7333-2017>, 2017a.
- 895 Liu, T., Liu, Q., Li, Z., Huo, L., Chan, M., Li, X., Zhou, Z., and Chan, C. K.: Emission of volatile organic compounds and production of secondary organic aerosol from stir-frying spices, *Science of The Total Environment*, 599–600, 1614–1621, <https://doi.org/10.1016/j.scitotenv.2017.05.147>, 2017b.



- Liu, Y., Ma, H., Zhang, N., and Li, Q.: A systematic literature review on indoor PM_{2.5} concentrations and personal exposure in urban residential buildings, *Heliyon*, 8, e10174, <https://doi.org/10.1016/j.heliyon.2022.e10174>, 2022.
- 900 Marć, M., Śmiełowska, M., Namieśnik, J., and Zabiegała, B.: Indoor air quality of everyday use spaces dedicated to specific purposes-a review, *Environmental Science and Pollution Research*, 25, 2065–2082, <https://doi.org/10.1007/s11356-017-0839-8>, 2018.
- Martin, W. J., Ramanathan, T., and Ramanathan, V.: Household Air Pollution from Cookstoves: Impacts on Health and Climate, in: *Climate Change and Global Public Health*, edited by: Pinkerton, K. E. and Rom, W. N., Springer International Publishing, Cham, 369–390, https://doi.org/10.1007/978-3-030-54746-2_17, 2021.
- 905 Marval, J. and Tronville, P.: Ultrafine particles: A review about their health effects, presence, generation, and measurement in indoor environments, *Building and Environment*, 216, 108992, <https://doi.org/10.1016/j.buildenv.2022.108992>, 2022.
- McLafferty, F. W. and Turecek, F.: *Interpretation of Mass Spectra*, 4th ed., University Science Books, Melville, 371 pp., 1993.
- Mohr, C., DeCarlo, P. F., Heringa, M. F., Chirico, R., Slowik, J. G., Richter, R., Reche, C., Alastuey, A., Querol, X., Seco, R.,
910 Peñuelas, J., Jiménez, J. L., Crippa, M., Zimmermann, R., Baltensperger, U., and Prévôt, A. S. H.: Identification and quantification of organic aerosol from cooking and other sources in Barcelona using aerosol mass spectrometer data, *Atmos. Chem. Phys.*, 12, 1649–1665, <https://doi.org/10.5194/acp-12-1649-2012>, 2012.
- Mohr, C., Huffman, A., Cubison, M. J., Aiken, A. C., Docherty, K. S., Kimmel, J. R., Ulbrich, I. M., Hannigan, M., and Jimenez, J. L.: Characterization of primary organic aerosol emissions from meat cooking, trash burning, and motor vehicles with high-
915 resolution aerosol mass spectrometry and comparison with ambient and chamber observations, *Environmental Science & Technology*, 43, 2443–2449, <https://doi.org/10.1021/es8011518>, 2009.
- Nasir, Z. A. and Colbeck, I.: Particulate pollution in different housing types in a UK suburban location, *Science of The Total Environment*, 445–446, 165–176, <https://doi.org/10.1016/j.scitotenv.2012.12.042>, 2013.
- Ng, N. L., Canagaratna, M. R., Zhang, Q., Jimenez, J. L., Tian, J., Ulbrich, I. M., Kroll, J. H., Docherty, K. S., Chhabra, P. S.,
920 Bahreini, R., Murphy, S. M., Seinfeld, J. H., Hildebrandt, L., Donahue, N. M., DeCarlo, P. F., Lanz, V. A., Prévôt, A. S. H., Dinar, E., Rudich, Y., and Worsnop, D. R.: Organic aerosol components observed in Northern Hemispheric datasets from Aerosol Mass Spectrometry, *Atmos. Chem. Phys.*, 10, 4625–4641, <https://doi.org/10.5194/acp-10-4625-2010>, 2010.
- Olson, D. A. and Burke, J. M.: Distributions of PM_{2.5} source strengths for cooking from the Research Triangle Park particulate matter panel study, *Environmental Science & Technology*, 40, 163–169, <https://doi.org/10.1021/es050359t>, 2006.
- 925 Omidvarborna, H., Kumar, A., and Kim, D.-S.: Recent studies on soot modeling for diesel combustion, *Renewable and Sustainable Energy Reviews*, 48, 635–647, <https://doi.org/10.1016/j.rser.2015.04.019>, 2015.
- Paatero, P. and Tapper, U.: Positive matrix factorization: A non-negative factor model with optimal utilization of error estimates of data values, *Environmetrics*, 5, 111–126, <https://doi.org/10.1002/env.3170050203>, 1994.
- Pope, C. A. and Dockery, D. W.: Health effects of fine particulate air pollution: lines that connect, *Journal of the Air & Waste Management Association*, 56, 709–742, <https://doi.org/10.1080/10473289.2006.10464485>, 2006.
- 930 Pope, C. A., Burnett, R. T., Thurston, G. D., Thun, M. J., Calle, E. E., Krewski, D., and Godleski, J. J.: Cardiovascular mortality and long-term exposure to particulate air pollution: epidemiological evidence of general pathophysiological pathways of disease, *Circulation*, 109, 71–77, <https://doi.org/10.1161/01.CIR.0000108927.80044.7F>, 2004.
- Reid, J. S., Koppmann, R., Eck, T. F., and Eleuterio, D. P.: A review of biomass burning emissions part II: intensive physical
935 properties of biomass burning particles, *Atmos. Chem. Phys.*, 5, 799–825, <https://doi.org/10.5194/acp-5-799-2005>, 2005.



- Reyes-Villegas, E., Bannan, T., Le Breton, M., Mehra, A., Priestley, M., Percival, C., Coe, H., and Allan, J. D.: Online Chemical Characterization of Food-Cooking Organic Aerosols: Implications for Source Apportionment, *Environmental Science & Technology*, 52, 5308–5318, <https://doi.org/10.1021/acs.est.7b06278>, 2018.
- Robinson, E. S., Gu, P., Ye, Q., Li, H. Z., Shah, R. U., Apte, J. S., Robinson, A. L., and Presto, A. A.: Restaurant Impacts on Outdoor Air Quality: Elevated Organic Aerosol Mass from Restaurant Cooking with Neighborhood-Scale Plume Extents, *Environmental Science & Technology*, 52, 9285–9294, <https://doi.org/10.1021/acs.est.8b02654>, 2018.
- Rogge, W. F., Hildemann, L. M., Mazurek, M. A., Cass, G. R., and Simoneit, B. R. T.: Sources of fine organic aerosol. 1. Charbroilers and meat cooking operations, *Environ. Sci. Technol.*, 25, 1112–1125, <https://doi.org/10.1021/es00018a015>, 1991.
- 945 Schneider, J., Weimer, S., Drewnick, F., Borrmann, S., Helas, G., Gwaze, P., Schmid, O., Andreae, M. O., and Kirchner, U.: Mass spectrometric analysis and aerodynamic properties of various types of combustion-related aerosol particles, *International Journal of Mass Spectrometry*, 258, 37–49, <https://doi.org/10.1016/j.ijms.2006.07.008>, 2006.
- See, S. W. and Balasubramanian, R.: Physical Characteristics of Ultrafine Particles Emitted from Different Gas Cooking Methods, *Aerosol Air Qual. Res.*, 6, 82–92, <https://doi.org/10.4209/aaqr.2006.03.0007>, 2006.
- 950 Shiraiwa, M., Ueda, K., Pozzer, A., Lammel, G., Kampf, C. J., Fushimi, A., Enami, S., Arangio, A. M., Fröhlich-Nowoisky, J., Fujitani, Y., Furuyama, A., Lakey, P. S. J., Lelieveld, J., Lucas, K., Morino, Y., Pöschl, U., Takahama, S., Takami, A., Tong, H., Weber, B., Yoshino, A., and Sato, K.: Aerosol Health Effects from Molecular to Global Scales, *Environmental Science & Technology*, 51, 13545–13567, <https://doi.org/10.1021/acs.est.7b04417>, 2017.
- Struckmeier, C., Drewnick, F., Fachinger, F., Gobbi, G. P., and Borrmann, S.: Atmospheric aerosols in Rome, Italy: sources, dynamics and spatial variations during two seasons, *Atmos. Chem. Phys.*, 16, 15277–15299, <https://doi.org/10.5194/acp-16-15277-2016>, 2016.
- Sun, Y.-L., Zhang, Q., Schwab, J. J., Demerjian, K. L., Chen, W.-N., Bae, M.-S., Hung, H.-M., Hogrefe, O., Frank, B., Rattigan, O. V., and Lin, Y.-C.: Characterization of the sources and processes of organic and inorganic aerosols in New York city with a high-resolution time-of-flight aerosol mass spectrometer, *Atmos. Chem. Phys.*, 11, 1581–1602, <https://doi.org/10.5194/acp-11-1581-2011>, 2011.
- 960 Thomas, R. J.: Particle size and pathogenicity in the respiratory tract, *Virulence*, 4, 847–858, <https://doi.org/10.4161/viru.27172>, 2013.
- Ulbrich, I. M., Handschy, A., Lechner, M., and Jimenez, J.L.: High-Resolution AMS Spectral Database, <http://cires.colorado.edu/jimenez-group/HRAMSsd/>, last access: 21 April 2022, 2022.
- 965 Ulbrich, I. M., Canagaratna, M. R., Zhang, Q., Worsnop, D. R., and Jimenez, J. L.: Interpretation of organic components from Positive Matrix Factorization of aerosol mass spectrometric data, *Atmos. Chem. Phys.*, 9, 2891–2918, <https://doi.org/10.5194/acp-9-2891-2009>, 2009.
- von der Weiden, S.-L., Drewnick, F., and Borrmann, S.: Particle Loss Calculator – a new software tool for the assessment of the performance of aerosol inlet systems, *Atmos. Meas. Tech.*, 2, 479–494, <https://doi.org/10.5194/amt-2-479-2009>, 2009.
- 970 Wallace, L. and Ott, W.: Personal exposure to ultrafine particles, *Journal of Exposure Science and Environmental Epidemiology*, 21, 20–30, <https://doi.org/10.1038/jes.2009.59>, 2011.
- Wallace, L. A., Emmerich, S. J., and Howard-Reed, C.: Source strengths of ultrafine and fine particles due to cooking with a gas stove, *Environmental Science & Technology*, 38, 2304–2311, <https://doi.org/10.1021/es0306260>, 2004.
- Wang, Q., He, X., Zhou, M., Huang, D. D., Qiao, L., Zhu, S., Ma, Y.-g., Wang, H.-l., Li, L., Huang, C., Huang, X. H. H., Xu, W., Worsnop, D., Goldstein, A. H., Guo, H., and Yu, J. Z.: Hourly Measurements of Organic Molecular Markers in Urban
- 975



- Shanghai, China: Primary Organic Aerosol Source Identification and Observation of Cooking Aerosol Aging, *ACS Earth Space Chem.*, 4, 1670–1685, <https://doi.org/10.1021/acsearthspacechem.0c00205>, 2020.
- WHO: Household air pollution, <https://www.who.int/news-room/fact-sheets/detail/household-air-pollution-and-health>, last access: 27 July 2023, 2022.
- 980 WHO: WHO global air quality guidelines: Particulate matter (PM_{2.5} and PM₁₀), ozone, nitrogen dioxide, sulfur dioxide and carbon monoxide, WHO European Centre for Environment and Health, Bonn, 285 pp., 2021.
- Williams, A., Jones, J. M., Ma, L., and Pourkashanian, M.: Pollutants from the combustion of solid biomass fuels, *Progress in Energy and Combustion Science*, 38, 113–137, <https://doi.org/10.1016/j.pecs.2011.10.001>, 2012.
- Wu, C. L., Chao, C. Y. H., Sze-To, G. N., Wan, M. P., and Chan, T. C.: Ultrafine Particle Emissions from Cigarette
985 Smouldering, Incense Burning, Vacuum Cleaner Motor Operation and Cooking, *Indoor and Built Environment*, 21, 782–796, <https://doi.org/10.1177/1420326X11421356>, 2012.
- Xu, J., Wang, P., Li, T., Shi, G., Wang, M., Huang, L., Kong, S., Gong, J., Yang, W., Wang, X., Geng, C., Han, B., and Bai, Z.: Exposure to Source-Specific Particulate Matter and Health Effects: a Review of Epidemiological Studies, *Curr Pollution Rep*, 381, 705, <https://doi.org/10.1007/s40726-022-00235-6>, 2022.
- 990 Xu, W., He, Y., Qiu, Y., Chen, C., Xie, C., Lei, L., Li, Z., Sun, J., Li, J., Fu, P., Wang, Z., Worsnop, D. R., and Sun, Y.: Mass spectral characterization of primary emissions and implications in source apportionment of organic aerosol, *Atmos. Meas. Tech.*, 13, 3205–3219, <https://doi.org/10.5194/amt-13-3205-2020>, 2020.
- Xu, W., Lambe, A., Silva, P., Hu, W., Onasch, T., Williams, L., Croteau, P., Zhang, X., Renbaum-Wolff, L., Fortner, E., Jimenez, J. L., Jayne, J., Worsnop, D., and Canagaratna, M.: Laboratory evaluation of species-dependent relative ionization
995 efficiencies in the Aerodyne Aerosol Mass Spectrometer, *Aerosol Science and Technology*, 52, 626–641, <https://doi.org/10.1080/02786826.2018.1439570>, 2018.
- Yeung, L. L. and To, W. M.: Size Distributions of the Aerosols Emitted from Commercial Cooking Processes, *Indoor and Built Environment*, 17, 220–229, <https://doi.org/10.1177/1420326X08092043>, 2008.
- Yin, J., Cumberland, S. A., Harrison, R. M., Allan, J., Young, D. E., Williams, P. I., and Coe, H.: Receptor modelling of fine
1000 particles in southern England using CMB including comparison with AMS-PMF factors, *Atmos. Chem. Phys.*, 15, 2139–2158, <https://doi.org/10.5194/acp-15-2139-2015>, 2015.
- Zhang, Q., Gangupomu, R. H., Ramirez, D., and Zhu, Y.: Measurement of Ultrafine Particles and Other Air Pollutants Emitted by Cooking Activities, *International Journal of Environmental Research and Public Health*, 7, 1744–1759, <https://doi.org/10.3390/ijerph7041744>, 2010.
- 1005 Zhang, Z., Zhu, W., Hu, M., Wang, H., Chen, Z., Shen, R., Yu, Y., Tan, R., and Guo, S.: Secondary Organic Aerosol from Typical Chinese Domestic Cooking Emissions, *Environ. Sci. Technol. Lett.*, 8, 24–31, <https://doi.org/10.1021/acs.estlett.0c00754>, 2021.
- Zhao, W., Hopke, P. K., Norris, G., Williams, R., and Paatero, P.: Source apportionment and analysis on ambient and personal exposure samples with a combined receptor model and an adaptive blank estimation strategy, *Atmospheric Environment*, 40,
1010 3788–3801, <https://doi.org/10.1016/j.atmosenv.2006.02.027>, 2006.
- Zhao, Y., Liu, L., Tao, P., Zhang, B., Huan, C., Zhang, X., and Wang, M.: Review of Effluents and Health Effects of Cooking and the Performance of Kitchen Ventilation, *Aerosol Air Qual. Res.*, 19, 1937–1959, <https://doi.org/10.4209/aaqr.2019.04.0198>, 2019.
- Zhao, Y., Hu, M., Slanina, S., and Zhang, Y.: Chemical compositions of fine particulate organic matter emitted from Chinese
1015 cooking, *Environmental Science & Technology*, 41, 99–105, <https://doi.org/10.1021/es0614518>, 2007.

<https://doi.org/10.5194/egusphere-2023-2172>

Preprint. Discussion started: 4 October 2023

© Author(s) 2023. CC BY 4.0 License.



Zhou, Z., Liu, Y., Yuan, J., Zuo, J., Chen, G., Xu, L., and Rameezdeen, R.: Indoor PM_{2.5} concentrations in residential buildings during a severely polluted winter: A case study in Tianjin, China, *Renewable and Sustainable Energy Reviews*, 64, 372–381, <https://doi.org/10.1016/j.rser.2016.06.018>, 2016.